PEER-TO-PEER 3D/MULTI-VIEW VIDEO STREAMING

by

Yan Ding

B.Sc., Zhejiang University, 2007

A THESIS SUBMITTED IN PARTIAL FULFILLMENT
OF THE REQUIREMENTS FOR THE DEGREE OF
MASTER OF APPLIED SCIENCE
in the School
of
Computing Science

APPROVAL

Name:	Yan Ding
Degree:	Master of Applied Science
Title of Thesis:	Peer-to-peer 3D/multi-view video streaming

Examining Committee: Dr. Arrvindh Shriraman
Assistant Professor of Computing Science
Chair

Dr. Jiangchuan Liu
Senior Supervisor
Associate Professor of Computing Science

Dr. Mohamed Hefeeda
Supervisor
Associate Professor of Computing Science

Dr. Jian Pei
Internal Examiner
Associate Professor of Computing Science

Date Approved:

Abstract

The recent advances in stereoscopic video capture, compression and display have made 3D video a visually appealing and costly affordable technology. More sophisticated multi-view videos have also been demonstrated. Yet their remarkably increased data volume poses greater challenges to the conventional client/server systems. The stringent synchronization demands from different views further complicate the system design. In this thesis, we present an initial attempt toward efficient streaming of 3D videos over peer-to-peer networks. We show that the inherent multi-stream nature of 3D video makes playback synchronization more difficult. We address this by a 2-stream buffer, together with a novel segment scheduling. We further extend our system to support multi-view video with view diversity and dynamics. We have evaluated our system under different end-system and network configurations with typical stereo video streams. The simulation results demonstrate the superiority of our system in terms of scalability, streaming quality and dealing with view dynamics.

Key Words: 3D/Multi-view Video, Peer-to-Peer Network, Segment Scheduling

Acknowledgments

Firstly I would like to show my deepest gratitude to my senior supervisor, Dr. Jiangchuan Liu for his continuous support and encouragement over these years. Through each insightful discussion with him, I learnt the ways of thinking and doing research. It is his knowledge, patience and invaluable suggestions that help me finish this thesis.

I would like to thank my supervisor Dr. Mohamed Hefeeda and my examiner Dr. Jian Pei serving on my committee and reviewing my thesis. I would like to thank Dr. Arrvindh Shriraman for taking the time to chair my thesis defense.

I would like to thank all my colleagues in our Multimedia and Networking Group for their kindness and help on my academic work and studying life.

Finally, I would like to thank my whole family for their endless love, support and encouragement. I would not have made it without them. This thesis is dedicated to them.

Contents

List of Tables

List of Figures

Chapter 1

Introduction

1.1 Introduction

The recent advances in stereoscopic video capture, compression, and display have made 3 Dimensional (3D) video a visually appealing and costly affordable technology. We have witnessed a series of new releases of 3D movies in the past two years (e.g., Avatar), with much more being just announced. FIFA, partnered with Sony, deliver 3D videos from 25 matches of the 2010 World Cup in South Africa, debuting a technology breakthrough in the broadcast history. The abundant content, together with the dramatically decreasing price, have become driving forces to the vast growth of 3D-capable disc players and LED TVs, or even notebooks (e.g., Toshiba Satellite A665) in the market, which are quickly sweeping away the conventional 2D devices.

3D video (also referred as *stereo* Video) is perceived by humans with additional three-dimensional depth, which is resulting from the spatial disparity of two slightly different streams for left and right eyes' viewpoints respectively. Currently, the popular H.264/AVC coding standard has well supported 3D video through its MVC (Multiple Video Coding) extension [42]. Beyond local storage and playback, faster home broadband connections have also fostered 3D video streaming over the Internet. Cisco predicted that 3D and high-definition video will increase 13 times between 2009 and 2014. By 2014, annual global IP traffic would reach almost three-fourths of a zettabyte (i.e., 0.75 trillion gigabytes), and 3D and high-definition video would comprise about 42% of it. The most popular video sharing site, Youtube, has promoted to develop a stereoscopic player since July 2009, and is currently experimenting over 100 experimental 3D videos supporting ten viewing styles.

There have been a number of pioneer academic works on streaming 3D video over the Internet, too; see [32] [41] [30]. Most of them, like those commercial products, are client/server based however. This classical communication paradigm has already suffered from streaming the traffic-intensive 2D videos, and the remarkably increased data volume of 3D videos poses even greater challenges. Peer-to-peer (P2P) streaming, on the other hand, has shown to be a highly scalable and practical alternative [38]. We believe that it can be a candidate of great potentials for 3D video streaming as well, particularly considering that its commercial success in delivering live TV or on-demand movies, and many these contents are in the transition from 2D to 3D.

The inherent multi-stream nature of 3D video unfortunately makes segment scheduling more difficult than that of 2D video, which has already been proved to be NP-Complete problem [62]. This is because, to enable stereoscopic perception at the user side, not only segments in one stream have to arrive before playback deadlines, but also they have to be paired with corresponding segments with the same playback time in the other stream. Poor synchronization between streams prolongs the playback delay, and would even cause spatial displacement of objects in the two views, resulting in false parallax perception [48]. The problem is severe in a peer-to-peer overlay, given the existence of multiple senders and node churns. For multi-view video, since a user is only interested in a subset of the views but can switch over views, the challenge becomes even acuter with such view diversity and dynamics.

In this thesis, we focus on the stereo segment scheduler design, a key component for streaming 3D/multi-view videos over P2P systems. The thesis has the following contributions:

- We present an initial attempt toward efficient streaming of 3D/multi-view videos over a P2P network. We show that the separated streaming brings comparable streaming service (higher streaming rate, lower startup delay and smoother playback) of the mixed streaming, with lower system cost and better scalability (lower server load).

- We show that the inherent multi-stream nature of 3D video makes segment scheduling more difficult, particularly, we formulate the stereo segment scheduling problem as a Binary Quadratic Programming (BQP) problem and discuss its hardness.

- We develop two efficient algorithms to allow peers frequently update the scheduling, and provide theoretical analysis on their performance guarantee and time complexity.

- We implement the optimal algorithm, the proposed algorithms in a large-scale P2P simulating system. Through simulation on typical stereo video sequence, we show that the proposed algorithms achieve near-optimal performance. Further comparison with other heuristic algorithms is also conducted, and the results demonstrate the superiority of our algorithms.

- We extend our algorithm to stream multi-view stereo video with video diversity and dynamics. To support it, a light-weight clustering based overlay is introduced. Under different end-system and network configurations with typical multi-view video sequence, we show that the designed overlay outperforms random overlay in efficient grouping/re-grouping peers in multi-view video.

1.2 Thesis Organization

This thesis is organized as follows. The background and related work is reviewed in Chapter 2. In Chapter 3, we present the proposed P2P 3D/multi-view streaming system, in particular, we discuss the stereo segment scheduling problem and algorithms/analysis, followed by the extension to support multi-view video. Evaluation and analysis for both the stereo and multi-view video streaming are presented in Chapter 4. Finally, we present the future work and conclude the thesis in Chapter 5.

Chapter 2

Background and Related Work

In this chapter, we give an overview of the peer-to-peer networks, in particular, the peer-to-peer file sharing and media streaming applications. We describe the features as well as the technical issues/challenges imposed in these applications. We focus on the on-demand video streaming and discuss the segment scheduling design issue. For 3D/mulit-view videos, we present a brief overview of the state-of-the-art its generation, encoding/decoding and display techniques, and streaming challenges, particularly the media synchronization. Finally, we present some related work.

2.1 Overview of Peer-to-Peer Networks

Peer-to-peer (P2P) networking provides an alternative to the traditional client/server architecture. In a client/server model, the clients make requests to the server with which they are networked with. And the server, typically an unanticipated system, responds to the requests from clients. With P2P networking, each participating computer (referred as a peer) has an additional layer of server functionality. This allows the peer to serve as both a client and as a server within a given application. Examples of P2P applications that are build on such an architecture are storage, content sharing and media streaming. Figure 2.1 illustrates the differences between client/server and P2P models. As we see that in client/server model, all the communications are controlled and coordinated by the central server, while in P2P model, communications go through and managed by peers directly. These exchanges include the control messages (such as requests for information of the content and file, computation to be performed, local knowledge to be distributed) and the real data transmission. Most of

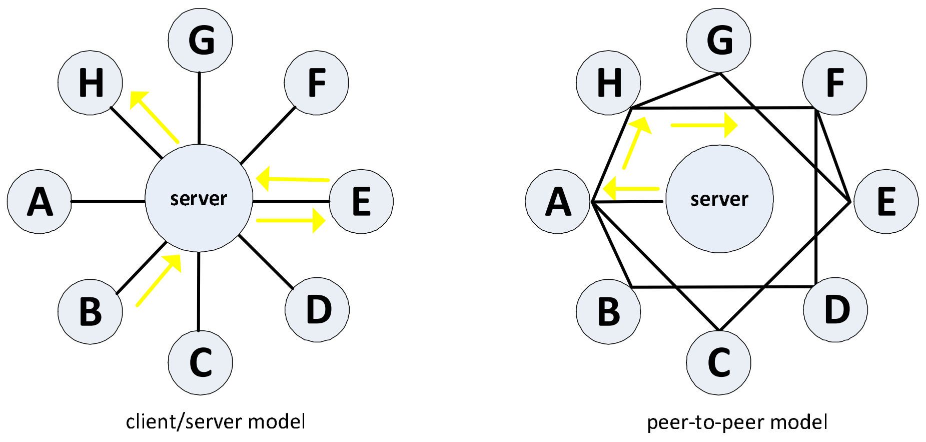

Figure 2.1: Client/server model and P2P model

P2P networks also require the server to perform some functions (e.g., for the content sharing and media streaming applications, the server is where all of the available files are initially stored), but the overall functionality of P2P networking is to distribute the computing to the edge of the network.

The use of P2P networking benefits both the service provider and participating clients. At the client side, the single-source bottleneck is eliminated. In the occurrence of server resource overwhelming or the connection failure, the ability of making direct exchange among other users liberates P2P clients from the traditional dependency on the central server. On the other hand, the costly data computation could be distributed to the clients to alleviate the server load and eliminate the risk of server death. This is particularly true for the large-scale communication network with millions of coexisting clients.

The most widely deployed P2P applications are the file sharing and media streaming systems. The file sharing is used for storing and distributing files among peers and the media streaming consists of live and on-demand video (VoD) streaming. We briefly overview these applications in the next two sections, and for VoD streaming that we are interested in this thesis, we give a more detailed design issues/challenges in section 2.1.3

2.1.1 File Sharing

In the file sharing application, users start to use the file after downloading the entire content. The most successful examples are the BitTorrent [1] and Gnutella [2]. Such systems provide users with potentially unlimited storage capacity by taking advantage of the content redundancy. Basically, the resource of the file is originally located at some peers in the application community, which is available to all of the participating users. Upon a user's request, the reference to the requested file will help the user find the resource peers from whom it can then download the file from.

The key technical issues imposed in such systems are network bandwidth consumption, security and fairness. The new demand of big object (e.g., the video, audio, software, other documents) and increased perception quality (e.g., high definition video, 3D/multi-view videos) requires much higher bandwidth consumption for downloading than traditional small objects such as files and music clips. The security issue arises due to the anonymity of participating users, and the unfairness comes from the existence of free riders, who utilize the system resource to get benefits without any contribution. This will degrade system scalability if a bunch of free riders exist. Some incentive mechanisms are developed to encourage contribution based on a so-called "tit-for-tat" strategy, which provides higher downloading speed to peers who have more bandwidth contributed [38].

2.1.2 Live and On-Demand Streaming

The media streaming applications are classified into two categories, namely, the live (PPLive [6], and UUSee [7]) and on-demand streaming (GridCast [12] and Vanderbilt VoD [11]). In P2P live streaming, the video source is freshly generated at the server and simultaneously streamed to current peers. This means that all peers are watching the same part of the video at the same time. The common interest of peers will increase the video content overlap and encourage resource sharing among them. However, this application comes across one more challenge (besides those in the file sharing) of minimizing the streaming delay, specially when millions of users request to join the system at a same very short time period (the problem is known as "flash crowd" [34]) since for live video streaming, failing to stream in real time will annoy watching users (e.g., the live broadcast of World Cup).

Compared with file sharing and live streaming, VoD generally supports richer user interactions, and users have limited content in common (since users can join in the system at any time and watch any part of the video). P2P VoD thus faces much more challenges, and existing solutions are yet to be perfected to compete with the conventional client/server model. In particular, it is well-known that the startup delay of state-of-the-art P2P VoD remains much longer than powerful client/server-based systems, particularly those with

Content Distribution Network (CDN) support. For example, for the on-demand mode in PPLive, the startup delays are often longer than 10 seconds, and sometimes go beyond half a minute, while the average delay of YouTube is about 6.5 seconds [47], though the latter has already been ranked as a slow site. The situation is only getting worse when rich VCR operations such as fast forward, rewind, and random seek are introduced.

2.1.3 Overlay Construction and Segment Scheduling

A P2P overlay network refers to an application-layer network consisting of all participating peers as the network nodes. Each overlay link that connects two peers is a logical link that is build on the top of the underlying physical network topology but not necessary depends on it. Such overlays are used for indexing and peer discovery for the desired files. The overlay construction can be classified into two categories, the structured overlay and unstructured overlay according to how the peers in the overlay network are linked to each other. The structured overlay enables a more structured pattern of the overlay link that allows peers to efficiently issue a search to some peer that has the desired file. The typical construction is the distributed hash table (DHT) indexing which uses a consistent hashing to allocate the ownership of each file to some particular peers, see example systems Chord [50] and CAN [46].

The unstructured overlay is however organized with overlay links arbitrarily established. Such overlays are quite easy to be constructed upon a newly joining or a leaving peer, e.g., when a peer firstly joins the overlay, it can directly fetch the overlay links from some existing peers, and when a peer leaves, it can simply delete its owning links without any influence on the remaining network. When a peer searches some file, it has to distribute the query in a flooding fashion until the desired file is located. Such an operation is quite costly for the rare content or the search could be highly possible to be unsuccessful when the content is only shared by few peers in the overlay since no correlation between the file and the peer is managed by any mechanism. Besides, the flooding can further increase the traffic throughout the overlay and thus decrease the bandwidth utilization. Although the structured P2P overlay provides efficient locating for both the popular and rare files, it introduces significantly higher maintenance overhead than the unstructured overlay for the popular contents. This is the main reason why the unstructured overlay is more widely used over the Internet today. A more detailed and complete survey of the structured and unstructured overlays is presented in [39].

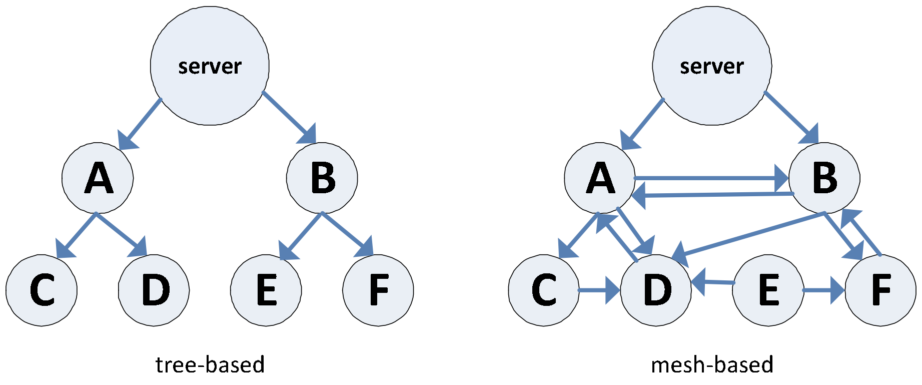

Figure 2.2: Tree-based and mesh-based data dissemination

In the unstructured overlays, there are two categories of approaches for data dissemination, namely tree-based and mesh-based (as illustrated in Figure 2.2), see the review in [38]. In the tree-based approach, peers are organized into one tree or multiple trees, with each data packet being disseminated through them. Peers in the tree(s) have well-defined relationship (i.e., parent-children relationship), where upon receiving one packet, the peer will forward the copies of the packet to all its children (called `Push` operation). Since all the data packets follow the same dissemination pattern, the tree(s) can be optimized to guarantee good streaming performance. However, as the majority of the peers reside in the leaves of the tree, their upload resources are not utilized efficiently. Further, such tree(s) are fragile particularly when a peer higher in the tree leaves or fails, it may disrupt delivery of data to a large number of offspring peers. To improve the resilience of the data delivery, the mesh-based approach is proposed, where no specific structure of date delivery is defined. Instead, peers randomly select some other peers to establish partnership to transmit data. The data transmitted is also determined by the receiving peer, which we refer this as *data-driven* or *receiver-driven* approach. The peer then fetches the desired data (called `Pull` operation) from partners according to the scheduling mechanism.

When the partnership is established, the scheduling algorithm is to determine which data segment should be fetched from which partner. The real time constraints in the media streaming applications imply that the data segments must be obtained in a timely manner, which thus requires the scheduling to fetch data segments from partners to meet their playback deadlines. Figure 2.3 shows the basic scheduling scheme for peer **D** in Figure 2.2, where a sliding buffer window is maintained, which indicates local segment availability

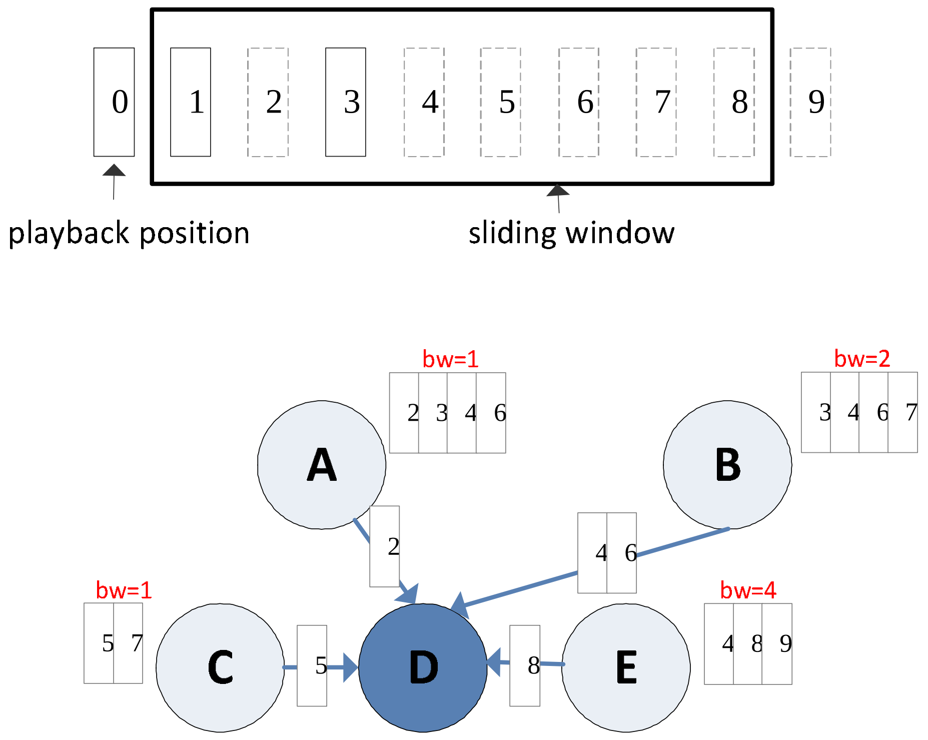

Figure 2.3: (a) Peer **D**'s sliding buffer window (segments with solid lines are available in the local buffer, and those with dotted lines are not); (b) **D** schedules missing segments from partners **A**, **B**, **C** and **E** (each partner has its bitmap and available upload bandwidth)

information. The data availability information is used to generate a called bitmap which is periodically updated as the window slides and exchanged between partners. Given the limited bandwidth and segment availability from each partner, the scheduling will have to be optimized to meet both the deadline and the bandwidth constraints. The basic scheduling problem is a variation of parallel machining scheduling problem [62], which is known as NP-Complete problem.

2.2 3D/Multi-view Video

The recent advances in stereoscope video capture, compression and display have made 3D video a visually appealing and costly affordable technology. And the 3D video service is predicted to be the next big thing in entertainment field, and it has attracted interests from both the academic research and industrial development.

3D video is perceived by human beings with an additional three-dimensional depth, which results from two spatial disparity of two views, each presenting the view of one eye (Figure 2.4(a)). The multi-view video, on the other hand, enables multiple positions of watching the same video. This allows the viewer select or change the preferred view position to enjoy the video, not necessary in the front middle of the screen. Each view position provides either the traditional monoscope perception or possible stereo perception from adjacent two views [27]. In the following sections, we present an overview of the generation, encoding/decoding and display technologies for the two applications and the streaming challenges, in particular, the media synchronization between two view streams.

2.2.1 Generation, Encoding/Decoding and Display

To enable 3D perception, two separated videos are to be recorded by two spatially displaced cameras, each representing the viewpoint of one eye (Figure 2.4(a)). The raw data are then encoded by using a codec that supports stereo/multiview video coding. One popular candidate is the new H.264 Multiview Video Codec (MVC) [42], which substantially extends the previous standard H.264 Advanced Video Codec (AVC) by exploiting the redundancy across different views. In the stereoscopic 3D case, one of the two videos is selected to be the reference view (e.g., the left video), and is encoded by the traditional H.264/AVC codec using motion compensation prediction (MCP) to explore the temporal redundancy within the view. The second view, which has high inter-stream correlations with the reference view, is encoded with newly developed disparity compensation prediction (DCP). Unlike MCP, the frame disparity in DCP does not come from temporal changes, but rather from the distance between the scene and the camera (d_2), as well as the displacement from one camera to another (d_1 in Figure 2.4(a)).

A typical MCP/DCP based encoding outcome is illustrated in Figure 2.4(b) (similarly, an example of multi-view prediction structure can be found in [28]). The dependency of the frames have been indicated through arrowed lines. The encoded frame data together with the auxiliary information (e.g., the view ID and prediction mode) will be encapsulated into independently decodable NAL (Network Abstraction Layer) units [58], which will be further encapsulated in RTP packets for real-time streaming. At the user side, the received data will be properly displayed by the visualization system. For example, users can wear shutter glasses to have stereoscope perception or install the more advanced additional hardware to automatically display stereo/3D videos.

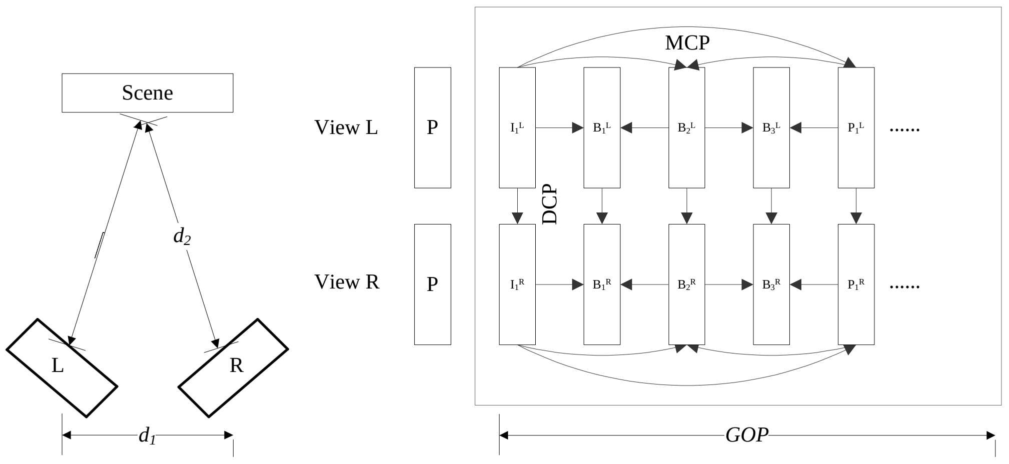

(a) 3D video generation (b) An illustration of MCP/DCP 3D encoding

Figure 2.4: 3D video generation and encoding

2.2.2 Media Synchronization

A critical issue in 3D video streaming is the coordination and synchronization of two view streams for the same video program [23]. Differently from the scalable video (SVC [15]) and multiple description video (MDC [14]), where the receiver can still play the video with considerable amount of layers (in SVC) or descriptions (in MDC) received, the tightly-coupled nature of the two streams in 3D video implies that, missing data segment from either one of the two streams will disrupt the normal playback. The coordination and synchronization can be considerably more complicated in P2P networks with each peer being both client and sever. In this thesis, we focus on the stereo segment scheduling to achieve synchronization between two streams.

2.3 Related Work

There have been significant studies on P2P video streaming in the past decade, leading to a number of successful products with large user bases. The general focus of this field has been largely on two issues, namely, overlay construction and data segment scheduling[38]. Both tree-based (e.g., NICE[9], ZigZag[53] and ChunkSpread[54]) and mesh-based (e.g., CoolStreaming[62] and PRIME[40]) overlay construction have seen real deployment, with mesh-based overlay being particularly popular among industrial products given its simplicity and robustness. Later works (e.g., [55], [54]) also seek hybrid designs that leverage the advantages of both.

Given an overlay structure, scheduling algorithms for each peer's buffer are then invoked to maximize the data delivering quality, particularly for mesh overlays with multiple neighboring peers. Work in [37] did a measurement-based study on random scheduling, and compared diverse elaborate and native scheduling schemes. A queue-based chunk scheduling strategy was then developed for live video streaming, which achieved a near-optimal streaming rate [16]. To enable efficient scheduling for both live and on-demand streaming, a more recent work was presented in [19], which theoretically formulated the scheduling problem, together with an approximation algorithm that maximizes the perceived video quality. Later ongoing efforts (e.g., [13] and [60]) further differentiated the strategies for data in a zone-based fashion. These previous works however considered scheduling the conventional single-view 2D video only. To our knowledge, P2P 3D video streaming has been largely unexplored. There have been a few related works for P2P streaming of other 3D contents, e.g., for virtual world [20] [51] [21]. A close work to multi-view video is [31], where video streams of multiple views are delivered over independent trees. We on the other hand considers the more practical mesh-based solution with a focus on the stereo segment scheduling to deliver different views.

With the recently advances in stereoscopic coding and displaying, 3D video streaming has received remarkable attention, too. A basic layered architecture of streaming stereoscopic videos over IP networks was outlined in [44]. To accommodate users with heterogeneous displays, a content-adaptive stereo video coding and streaming framework was presented in [8]. User interactivities in the multicast environment has also been examined in [29]. A critical issue in 3D video streaming is the coordination and synchronization of multiple streams for the same video program [23]. An early work in [43] presented a protocol for bandwidth aggregation and state exchange across multiple streams of a 3D video. It was later enhanced in [61] [59] through exploring semantic redundancies among multiple related streams, which better adapts to network dynamics. End-to-end rate-distortion optimization has been examined [52] through estimating both the data importance and the network link conditions. All the above works have relied on the classical client/server architecture, which is known to be non-scalable and the the sheer volume of 3D video data further aggravates the problem. Our focus is on P2P streaming, which we believe is a promising scalable solution for 3D videos. Yet given the inherent multicast nature and that each participating node can be both client and server, the coordination and synchronization can be considerably more complicated.

The multimedia synchronization problem for general distributed systems was studied since early 90s. The inter-media synchronization was examined in [49] from both operating system and parallel programming perspectives. An early synchronization control protocol for networked real-time data transmission was presented [35]. In [24], an adaptive timing across media outputs was developed for both tightly- and loosely-coupled streaming. Synchronization can also achieved by accelerating or retarding the media transmission on the server side [25], or alternatively by skipping or pausing the media presentation on the client side [17]. There have been a number of recent contributions, and a comprehensive survey that summarizes the traditional and state-of-the-art media synchronization approaches can be found in [10]. These works have largely concentrated on synchronization between video and audio (lip-syn) or text, and mainly in the client/server context. Similar work for the stream synchronization are P2P systems with SVC [15] and MDC [14]. As we stated previously, the receiver can still play the video with considerable amount of layers (in SVC) or descriptions (in MDC) received, the tightly-coupled nature of the two streams in 3D video will disrupt the normal playback by missing data segment from either one of the two streams. The coordination and synchronization can be considerably more complicated in P2P networks with each peer being both client and sever. This thesis work is motivated by these studies.

Chapter 3

P2P 3D/Mulit-view Streaming System

In this chapter, we present our peer-to-peer streaming system for 3D/multi-view videos. We start with an overview of our system model for 3D/stereo videos, and detail the design in the following two sections. In particular, we focus on the stereo segment scheduler design, where we mathematically formulate the scheduling problem and propose efficient algorithms. We will present extension of our design to support multi-view videos in Section 3.4 and some discussion in Section 3.5.

3.1 System Model

While existing 3D video streaming systems are generally client/server based, this conventional architecture has already suffered from streaming traffic-intensive 2D videos, and the remarkably increased data volume of 3D video poses even greater challenges. Peer-to-peer streaming, on the other hand, has shown to be a highly scalable and practical alternative. We believe that it can be a candidate of great potentials for 3D video streaming, too, particularly considering that its commercial success in delivering live TV or on-demand movies, and many these contents are in the transition from 2D to 3D.

We advocate a mesh-based P2P streaming system, which has been widely used in state-of-the-art commercial systems [62] [6]. Each newly joined client (peer) will be informed with a list of active peers interested in the current video, and it will randomly select some of them to establish partnerships. It will then exchange bandwidth and data availability information with these partners and fetch video data through a scheduler, which specifies each partner to transmit which segments. The active peer list will be periodically gossiped through the overlay, so that existing peers can update their partners to accommodate peer and network dynamics and possibly achieve better streaming performance.

Differently from traditional monoscopic 2D video streaming, two distinct data sequences for a 3D video will be distributed, which are correspondingly produced by the encoded left and right views. Data segments with the same playback time, upon receiving, will be combined to produce a *stereo frame pair*, enabling depth perception. To ensure that the segments of different views arrive simultaneously at a destination, a simple approach would be mixing the segments into one streaming for transmission. It is however quite inflexible, and we instead suggest that the segments being delivered through two separate streams. A salient advantage here is the better compatibility and interoperability with monoscopic-only clients, since only one of the two streams is needed given the client's bandwidth or display device constraints. This is necessary for a smooth and therefore successful transition to 3D video from the current hardware and software platforms that remain dominated by 2D video.

The use of separate streams unfortunately makes segment scheduling more difficult. The situation becomes particularly severe with the existence of multiple senders as both the sending time and the traveling duration would vary in the presence of network dynamics. Poor synchronization prolongs the playback delay, and would even cause spatial displacement of objects in the two views, resulting in spatial displacement of objects and false parallax perception [48]. We will describe the 2-stream buffer to accommodate stereo segments, and the stereo segment scheduler design to facilitate both intra-stream continuity and inter-stream synchronization. That is, data segments within the same stream have to be received before their deadlines, and meanwhile they have to be paired with the corresponding segment in another stream. Note that we focus on the segment scheduler design, which is a key component in P2P streaming systems. Our solution however does not impose any assumption on other components in the system, and therefore, it can be easily implemented in the current mesh-based P2P systems to support stereo video streaming.

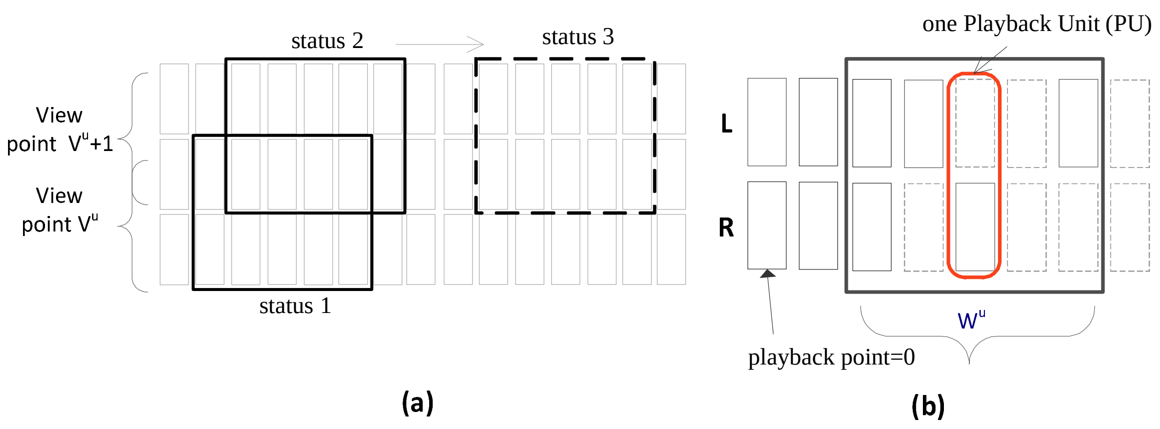

Figure 3.1: 2-stream buffer: (a) User changes viewpoint from i to $i + 1$ (status $1- > 2$), and stays watching (status $2- > 3$); (b) Buffer details for a fixed viewpoint (segments with solid lines are available in the local buffer, and those with dotted lines are not)

3.2 Buffer Management

As in other mesh-based overlays, each peer in our system maintains a buffer for the received video segments, and a window slides over the buffer, covering the segments of interest for playback and transmission. The availability of the segments within the window is represented by a peer's buffer bitmap, which is periodically updated and exchanged among partner peers.

Differently from conventional 2D video streaming, for stereoscopic 3D videos, each peer's local buffer has to maintain two separated lists, each stores the received segments from one view. Peer's buffer status is represented by its value of *center-of-interest*(`COI`) expressed as `COI(time, viewpoint)`, representing which viewpoint and which part of video it is currently watching. The `time` is set to be in the middle of the sliding window and the `viewpoint` represents which two views constitute the stereoscope perception. After `COI` values are distributed, peers will find interested partners, and establish partnerships for data exchange.

Fig.3.1(b) shows an example of peer's buffer window, which indicates the received and absent segments from both two views. A *playback unit* (PU) (also referred as a segment pair) consists of one left segment and one right segment with the same playback time. Missing either one will result in discontinued playback, or renders the view to be monoscopic, which is undesirable for 3D-capable viewers.

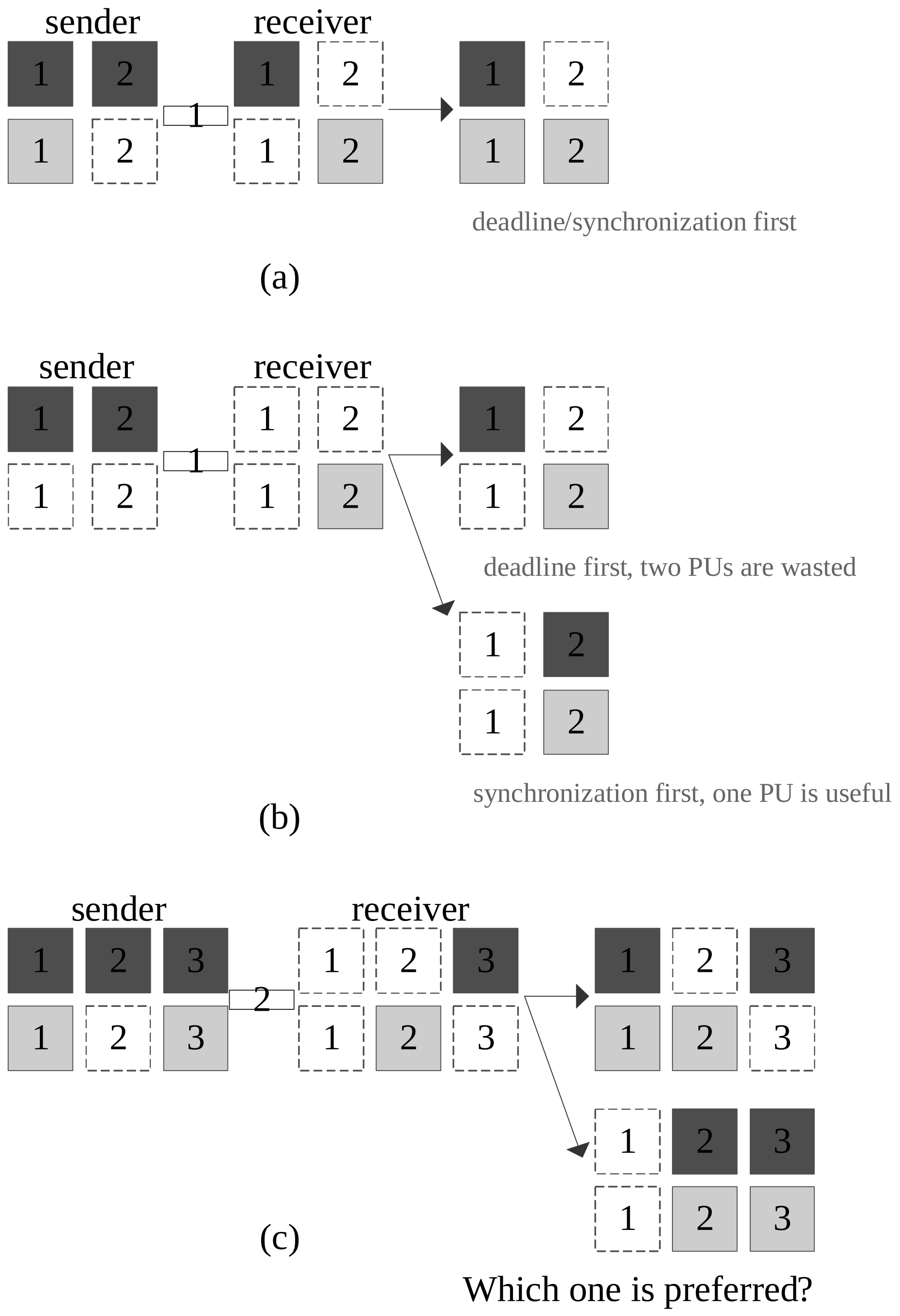
sender
receiver
1
2
deadline/synchronization first
(a)
deadline first, two PUs are wasted
synchronization first, one PU is useful
(b)
3
(c)
Which one is preferred?

Figure 3.2: Cases of 2-stream buffer scheduling

Figure 3.2 shows an example of the difficulty of stereo segment scheduling (with coexistence of playback deadline, limited bandwidth, availability and stream synchronization) with the 2-stream buffer, where the peer receiver has only one sender. The dark grey segments are from stream 1 and the light grey ones are from stream 2. The blank ones are missing segments. There are links between sending and receiving peers with a number on it, indicating the uploading bandwidth (or the maximum number of segments that can be transmitted within one time slot).

- In case (a), only one segment can be transmitted. Obviously, segment1 from stream2 should be fetched for it has earlier deadline, and also it can compose a complete PU.
- In case (b) with the same available bandwidth, there are however two options, as shown in Figure 3.2. The second one is preferred since there will be at least one PU useful, although it does not obey deadline-first.
- A more complicated situation is shown in case (c). In the first option, the scheduler fetches the two segments with the earliest deadlines, which also constitute a useful PU, while in the second option, it selects later segments but can obtain two useful PUs.

The question arises: which one should the scheduler prefer, deadline first with fewer useful PU or more complete PUs with urgent segments left missing? The situation could be further complicated when more senders are involved.

3.3 Stereo Segment Scheduling

We now mathematically formulate the stereo segment scheduling as an Binary Quadratic Programming problem, and show its hardness. We will present the two proposed algorithms to achieve efficient scheduling, followed by the algorithm analysis.

3.3.1 Problem Statement

Let PU^u denote the set of PUs to be scheduled for u (since peers only schedule segments within the buffer window, the maximum number of PUs equals peer's window size, which is W^u). Let w_i denote the weight of the i^{th} PU and O be u's partner set ($|O| = M$). We use V^u to denote u's views set, $V^u = \{L^u, R^u\}$, meaning that u's stereoscope viewpoint is composed of the left view L^u and the right view R^u. The segment availability in partner m is represented by $a^m_{ik_u}, k_u \in V^u$, indicating whether m has buffered the i^{th} segment of stream k_u (with $a^m_{ik_u} = 1$ being yes). Let b^{mu} denote m's bandwidth allocated to u. In our system, each partner will evenly allocate its total bandwidth to all its receiving peers for fairness. Let $x^m_{ik_u}$ denote the scheduling variable, representing whether fetching the i^{th} segment of stream k_u from m or not. We formulate the stereo segment scheduling problem as follows:

$$Max. \quad \sum_{i \in PU^u} w_i \prod_{k_u \in V^u} x_{ik_u} \tag{3.1}$$

$$s.t. \quad x_{ik_u} = \sum_{m \in O} x^m_{ik_u} + a^u_{ik_u} \tag{3.2}$$

$$x^m_{ik_u} \leq a^m_{ik_u}, k_u \in V^u \tag{3.3}$$

$$\sum_{k_u \in V^u} \sum_{i \in PU_u} x^m_{ik_u} \leq b^{mu} \tag{3.4}$$

$$\sum_{m \in O} x^m_{ik_u} \leq 1 \tag{3.5}$$

$$x^m_{ik_u}, a^m_{ik_u} \in \{0, 1\} \tag{3.6}$$

The objective function is to maximize the weighted number of complete PUs. The weight w_i could be modeled as the importance of the i^{th} PU (e.g., video quality improvement, the decoding role it takes, or the urgent level it lies (deadline related)). We will discuss the weight modeling issues in Discussion Section. The first constraint means that any segment is only available if at least one of the partners send it to u, or u has already locally buffered it. The second constraint implies that whether the sending partner m has a copy of this segment or not. The third constraint indicated the bandwidth limitation. Note that b^{mu} is represented by the number of segments. This is an approximated value since segments have different sizes. However, upon receiving transmission requests, partners will send segments until total bandwidth is used up. The fourth constraint is to avoid duplicated transmission from multiple partners.

Problem Hardness and the Optimal Solution: The stated stereo segment scheduling is Binary Quadratic Programming (BQP) problem, which is known to be NP-Hard [26]. Many existing solvers are developed to optimally solve these problems. In this thesis, we implement the MIQP solver in CPLEX [3] package to get the optimal scheduling (referred as OPT algorithm), serving as the benchmark for performance comparison.

Table 3.1: Notations in BMF algorithm and their definitions

Notations	**Definitions**
$^{(m)}$	the m^{th} round
$A^{(m)}$	scheduling strategy
A_{km}	segment pairs of k and m
$b_k^{(m)}$	k's remaining bandwidth
B_k	partner k's bitmap
K	set of successfully matched partners
N_{km}	maximum number of pairs matching k and m
$N^{(m)}$	total number of scheduled pairs
w_i	weight of the i^{th} pair
w_{km}^{+}	total increased weight of matching k and m
W^u	maximum number of pairs need to be scheduled for u
$pairs(k,m)$	total number of pairs from B_m and B_k

3.3.2 Algorithms and Analysis

The MIQP solver can get the optimal solution. However, given that the large scale and high dynamics nature of P2P network, as well as the stringent deadline requirement in VoD streaming, this method is too costly to be obtained in the real world implementation. We thus design two efficient heuristics to allow each peer (u) frequently update the schedule. The key observation is that partners are no longer independent with each other to make a valid contribution as that in 2D segment scheduling, but rather, each peer needs to be matched with another peer being its "collaborator" to transmit a complete segment pair (the i^{th} PU), with one contributing the left segment (i^{th} segment of stream L^u) and the other contributing the right one (i^{th} segment of stream R^u). Thus, our goal is to find out the best matchings of partners to transmit as highest weighted segment pairs as possible, given partners' limited bandwidth and segment availability.

Best Matching First (BMF) Algorithm: As the name indicates, the first algorithm is focused on the partner matching, where it processes partners sequentially. The main idea is, for each currently processing partner, BMF selects its best "collaborator" (in terms of the weight contribution they produce) among possible candidates to transmit segment pairs. For reference, we summarize the notations used in BMF and their definitions in Table 3.1.

The pseudo code of BMF algorithm (at peer u) is present in Algorithm 1. Basically, the scheduler runs totally M rounds, each processing one partner m. When processing m, the scheduler will search the whole set of candidates (partner 0 to m, line4), and select matching m with k that produce the highest sum of increased weight (line10, assume that the segment pair has been sorted with weight decreasing order, and we could then simply select the first N_{km} pairs to compute the increased weight, see line7,8). At the same time, the corresponding two partners (m and k) will have remaining bandwidth updated for future round's processing. Note that partner m can match with itself, in this case, the bandwidth update is done in line12, and for matching two different partners, see line15. Meanwhile, the scheduling strategy is updated as well as the total number of scheduled pairs (line17). It keeps searching for the second highest sum of increased weight, and so on until there are no segment pairs to fetch for m (line3). The situation occurs when partner m and k's upload bandwidth is used out ($b_k^{(m)} = 0$ or $b_m^{(m)} = 0$), or two partners cannot constitute any pair ($pairs(k, m) = 0$), or all of the missing pairs are already scheduled in previous rounds ($N^{(m)} = W^u$)(line6). Recall that the bandwidth is presented in terms of the number of segments. The matching result comes from processing partners' bitmaps (e.g., do AND operation), which will be iteratively updated by the newest scheduling strategy $A^{(m)}$ (line5). This operation is to avoid duplicated segments transmission from multiple partners. The reason why we only need to update m's bitmap is because previously searched candidate $k \in K$ will no longer be considered to match with m since they have already constitute pairs before (line4). The final scheduling ($A^{(M)}$) will be conducted after all partners are processed.

With no further pairs to fetch, partners may still have remaining bandwidth. We utilize these resource to transmit as many single segments as possible since more fully filled local buffer will facilitate scheduling in the next time lot.

The time complexity of BMF is $O(M^3N)$, where M is the total number of partners and N is the total number of segment pairs. In typical P2P systems, each peer maintain approximately tens of partners and each time slot only needs to process tens of segment pairs. Therefore, the running time is very small and practical for the real time implementation. BMF guarantees optimum up to the current processing round. However, it may not necessarily bring the global optimum since later partner information is not considered for the current round. Further, it has no performance guarantee due to the various partner ordering since the scheduling sequentially processes one partner to another (for example, sorting partners with bandwidth decreasing order may take better advantage of upload resources, and sorting them with fewest number of available segments may successfully fetch rare segments to compose high-weight pair. We will examine the impact of partner ordering in evaluation chapter).

Algorithm 1: BMF: Best Matching First Algorithm

```
1  for $m = 1$ to $M$ do
2      $A^{(m)} = A^{(m-1)}$, $N^{(m)} = N^{(m-1)}$, $b_k^{(m)} = b_k^{(m-1)}$, for $k = 0, 1, ..., m$
3      while $N_{k'm} > 1$ do
4          for $k = 0$ to $m$ AND $k \notin K$ do
5              update $B_m \leftarrow A^{(m)}$
6              $N_{km} = min\{b_k^{(m)}, b_m^{(m)}, W^u - N^{(m)}, pairs(k,m)\}$ for $k \neq m$, or
               $N_{mm} = min\{b_m^{(m)}/2, W^u - N^{(m)}, pairs(m,m)\}$
7              $A_{km} \leftarrow$ select first $N_{km}$ pairs from $B_k, B_m$
8              $w_{km}^{+} = \sum_{i=i_{N^{(m)}+1}}^{i_{N^{(m)}+N_{km}}} w_i$
9          end
10         $K \leftarrow k' = \arg\max_k w_{km}^{+}$
11         if $k = m$ then
12             $b_m^{(m)} = b_m^{(m)} - 2N_{mm}$
13         end
14         else
15             $b_m^{(m)} = b_m^{(m)} - N_{k'm}$, $b_{k'}^{(m)} = b_{k'}^{(m)} - N_{k'm}$
16         end
17         update $A^{(m)} \leftarrow A_{k'm}$, $N^{(m)} = N^{(m)} + N_{k'm}$
18     end
19 end
20 Do scheduling $A^{(M)}$
```

Highest-weighted Pair First (HPF) Algorithm: Differently from BMF, HPF processes segment pairs sequentially, starting from the pair with the highest weight and then the second highest and so on. As in Algorithm 2, we firstly sort all possible W^u segment pairs in weight decreasing order (line2). And for each segment pair i, the HPF scheduler will find two partners sets that can transmit i's left segment and right segment respectively (line6,9). Then it randomly selects two partners (m^L and m^R), each from one set, that can collaboratively transmit a complete pair (line12) and schedule the corresponding segments to the two partners (line13). Meanwhile, their remaining bandwidth are updated (line14). Similarly, the scheduler stops when all of the required segment pairs are scheduled or any two of the partners can not transmit a whole pair (either they have no remaining bandwidth or they do not cache the segments in their local buffers), and does the scheduling (line16). In the following theorem, we prove that the proposed HPF algorithm has an approximation factor of 3 for the stereo segment scheduling problem.

THEOREM 1. *HPF has an approximation factor of 3 for the stereo segment scheduling*

Proof. Let P be the set of segment pairs scheduled by our algorithm and P^* be the optimal solution. Correspondingly, $W(P)$ is the total weight value HPF generates and $W(P^*)$ is the optimal value. We define $S = P \bigcap P^*$, $T = P \setminus S$ and $T^* = P^* \setminus S$. Therefore, we have $P^* = S \bigcup T^*$, where $S \subseteq P$. For each segment pair $i^* \in T^*$, which is scheduled to fetch from partner m_i^* and n_i^* in the optimal solution, the reason why our algorithm does not schedule it is because at least one of m_i^* and n_i^* has no remaining bandwidth (line5,8) when we are trying to schedule this pair (since it is in the optimal solution, the two partners do have cached the corresponding segments). Thus, the last remaining bandwidth of m_i^* or/and n_i^* must be used in some previous round in HPF to fetch another segment pair, say $j(i^*)$. By our algorithm (line2,3), the weight value produced by pair $j(i^*)$ is higher than i^*, that is, $w_{i^*} \leq w_{j(i^*)}$. Note that $j(i^*)$ could be in S. This case happens when HPF chooses two wrong partners (at least one of them are either m_i^* or n_i^*) to fetch it due to the random partner selection (line12), resulting in this partner's bandwidth unable to be used to fetch later segment pair. Thus, we have $j(i^*) \in P$. Note that for different i^*, we may have the same $j(i^*)$, however the number of copies of the same $j(i^*)$ is at most two since only two bandwidth is needed to fetch one pair, which implies that $\sum w_{j(i^*)} \leq 2 \sum w_j, j \in P$. Therefore, $W(P^*) = W(S) + W(T^*) = W(S) + \sum w_{i^*} \leq W(S) + \sum w_{j(i^*)} \leq W(P) + 2\sum w_j \leq W(P) + 2W(P) = 3W(P)$. □

Table 3.2: Notations in HPF algorithm and their definitions

Notations	**Definitions**
PU	segment pairs set
u	receiving peer
m	partner m
i	pair i
S_m	segments set scheduled for m
L_i	partners set of i's left segment
R_i	partners set of i's right segment
s_{iL^u}	i's left segment
s_{iR^u}	i's right segment

Algorithm 2: HPF: Highest-weighted Pair First Algorithm

```
1  $S_m = \emptyset$, for $m = 1, 2, ..., M$
2  Sort segment pairs in $PU$ with weight decreasing order
3  for segment pair $i \in PU$ do
4      for $m = 1$ to $M$ do
5          if $a^m_{iL^u} = 1$ and $b^{mu} > 0$ then
6              add $m$ to $L_i$
7          end
8          if $a^m_{iR^u} = 1$ and $b^{mu} > 0$ then
9              add $m$ to $R_i$
10         end
11     end
12     randomly select one partner $m^L$ from $L_i$, and one $m^R$ from $R_i$
13     $S_{m^L} \leftarrow s_{iL^u}$, $S_{m^R} \leftarrow s_{iR^u}$
14     update $b^{m^L u}$ and $b^{m^R u}$
15 end
16 Do scheduling $S_m$, for $m = 1, 2, ..., M$
```

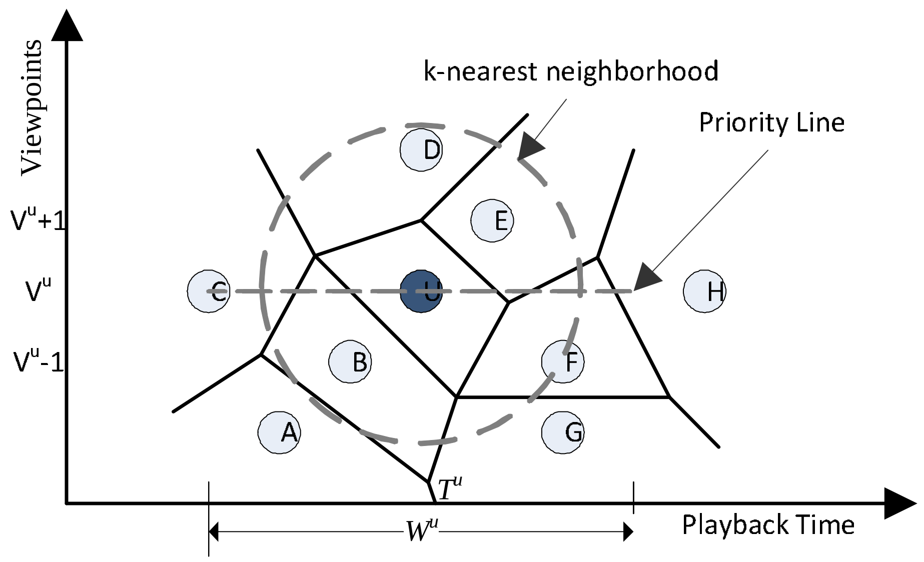

Figure 3.3: V-Plane Overlay: U has direct partners C in its *priority line*, and indirect partners B,D,E in its k-nearest neighborhood

The time complexity of HPF is $O(MN)$, where M is the total number of partners and N is the total number of segment pairs. Similarly as stated previously, as each peer maintain approximately tens of partners and each time slot only needs to process tens of segment pairs. Therefore, the running time is also very small. Further, HPF scheduler have partners load reasonably balance due to the randomness of selecting partners among possible candidates to transmit segments.

3.4 Extension to Multi-view

In this section, we implement our segment stereo scheduler in multi-view scenario to verify its feasibility, where to support multi-view with view diversity and dynamics, a light-weight clustering based overlay will be introduced.

To realize multi-view video, multiple cameras that are spatially displaced record the same video from one different angle, each representing a 2D viewing position. This allows users to arbitrarily select one viewpoint to enjoy the video, not necessary to be on a fixed position in the middle front of the screen. Further, users can possibly have 3D perception from two adjacent views in multiple different viewing positions, which we are interested in the thesis.

In this multi-view scenario, not only a user might be interested in different part of a video, but also might prefer to watch the video from different angles as well. This constrains resource sharing among peers. Besides the view diversity, users may change viewpoint during watching. Some pioneer work address this problem by view prediction from users feedback in clinet/server streaming. This is however computationally costly given the co-existence of millions of users as well as frequent view changes.

We address these challenges by leveraging clustering (in particular, Voronoi diagram [33]) to efficiently locate partners with same/overlapped interest. As in Fig.3.3, we use Voronoi diagram as a virtual plane (called V-Plane) that extends in time and space dimensions. The space dimension consists of discrete viewpoints, each representing a 3D perception of two adjacent views. The time dimension then corresponds to playback time slots. As such, each peer can be located at one point in the V-Plane according to its `COI` value (recall that the `COI` is the center of peer's interest, expressed as `COI(time, viewpoint)`). We can see that, although peers have individually-differentiated `COI`, they can still have overlapped content of interest. This is because peers are usually interested in video content in a period of time, which locate near its `COI` (in the time scale). Further, adjacent peers will have one same view shared (in the space scale). As an example, peer **A** with `COI(3,1)` and peer **B** with `COI(4,2)` both are interested in video segments playing at time 3 and 4 in view 2 (consider the buffer window of size 3).

In V-Plane, peers having overlapped interest are partners. Each peer maintains two partners lists, namely, direct partners (DP) and indirect partners (uDP). The DP list consists of partners that are watching at the same viewpoint and are within the interest time period (in peer's *priority line*, Fig.3.3), while the uDP list has partners locating at farther range (in peer's k-nearest neighborhood). Although the indirect partners may not exchange the current video content, they could be possibly promoted to be direct partners, especially when the peer changes viewpoint or when it has insufficient number of direct partners. An example of peer's direct and indirect partners is shown in the figure.

Note that with view dynamics, the 2-stream buffer window will slide in both spatial and temporal directions (Fig.3.1(a)). This means that in the case of view change, the pre-downloaded content of the current viewpoint may not be useful while the new content of interest has yet to be fetched. To avoid data outage, the V-Plane overlay reduces the view switching delay by quickly re-locating new partners; for example, when **U** changes perception viewpoint, it can quickly locate new direct partners from its current uDP list (since in the normal cases, peers will gradually change viewpoints, i.e., to its adjacent viewpoint first). View dynamics also implies frequent updates of `COI`. This will however introduce little computational overhead because, during the normal playback, both a peer and its partners' sliding windows are moving with the same speed (i.e., the video playback speed). Therefore, the partnership is maintained and no update is needed. Further, there is no data exchange between indirect partners, and thus, little more information (e.g., the bitmap) need to be maintained.

3.5 Discussion

In this section, we will discuss the weight modeling of PUs (segment pairs) and implementation issues on inter-operability of 3D/multi-view video with existing 2D videos.

The weight of each PU is an important factor in stereo segment scheduling. We currently integrate two factors to model the weight, namely, smoothness gain (SG) and quality gain (QG). The SG contribution of the weight comes from the playback upon receiving the complete PU, which is basically deadline-based. We model the smoothness gain as $SG = g(d)$, where d is the corresponding deadline and g is a monotonically decreasing function since urgent segments would bring relatively better continuity. QG presents the quality that PU brings. In video coding, a frame's quality is typically evaluated by its PSNR value. The computation of PSNR unfortunately requires full decoding of the received frame and the knowledge of the original frame values, which are hardly available during real-time streaming. The computation also involves intensive processing. Given that we are interested in the relative ranking of each frame, we instead examine how much possible quality degradation each frame would cause upon loss. A straightforward way is to use the accumulated bits to represent the quality degradation of the frame (equally the frame size), which we implemented in our scheduling for its simplicity and light computational complexity.

There are many advanced quality degradation modelings in the literature that are based on the distortion estimation upon frame loss, which considers both the decoding dependency and networking congestion. There are many pioneer work on this field, as mentioned in previous sections, state-of-the-art 3D encoding such as H.264 MVC explores both intra and inter view redundancy for compression. As such, the absence of a frame would render a series of frames to undecodable should they use this frame as a reference, within or across views. For example, in Figure 2.4(b), missing frame P_1^L will affect frame B_2^L, B_3^L and P_1^R, which will further affect the decoding of B_2^R and B_3^R. A dependency List (DL) of P_1^L can be defined to represent these affected frames. Consider a typical error concealment scheme upon loss, where the lost frame (say frame A) will be replaced by the previous successfully received frame (say frame B), and frames belonging to A's DL will also be replaced by B. We will then have an absolute Difference Value (DV) for each frame, which is computed as the sum of Mean Absolute Difference (MAD) of this frame and those in its dependency list. That is, for the n^{th} frame, we have $DV_n = \sum_{m=1}^{M} MAD_m, m \in DL_n$, where M is the length of frame n's DL. The DV value qualitatively characterizes the degradation upon loss of the frame, or equivalent, the gain if it were not lost. Thus, we can model the quality again for PU i being: $QG_i = \sum_{m=1}^{M} MAD_m, m \in DL_n, i \in$ frame n. The QG_i values can be generated during encoding at the server side, and are then distributed from the server to the whole overlay, so that all participating peers can have this knowledge for each PU.

A more accurate distortion estimation model is proposed in [57], given as $D_{c,n} = PD_{ECP,n} + \alpha(\beta_n, P)D_{c,n-1}$. The distortion of frame n is recursively computed as the sum of the concealment distortion in this frame and the channel distortion in the previous frame by a factor of α, which depends on the network loss probability P and the inherent encoding configuration β_n, e.g., the intraprediction ratio within one frame and the de-blocking filtering. This model considers the loss from the network congestion, the concealment error from reconstructing of the current encoded frame, and the error propagation from previously related frames as well. And thus, it provides more accurate estimation with sacrifice of increased computation cost since it requires per-pixel error computation and exploration of slice construction inside the frame at the server side, and these information has to be distributed among the whole network to allow local scheduling computation.

We now discuss some implementation issues on inter-operability of 3D/multi-view video with existing 2D videos. As 3D video remains in its early stage, many of the existing client video playback platforms support monoscopic 2D video only, even though a client may have sufficient bandwidth to receiving 3D streams. On the other hand, some 3D-capable client may want to disable it and instead have smoother 2D playback with less bandwidth demand. We thus believe that it is necessary to accommodate these clients in our 3D streaming system, so as to enable a smooth transition toward the full 3D peer-to-peer streaming.

Our separate stream design well supports such a compatibility mode. A traditional 2D client may simply fetch and playback one view only, and use extra bandwidth, if available, to assist the streaming of another view. Note that, if the two views are independently encoded, the client can arbitrarily choose one. For H.264 MVC-like encoding, however, inter-view redundancy is explored and there is a reference view (MCP-coded) for decoding of other views. In this case, the 2D client need to fetch and display this reference view only. Alternatively, the client may fetch certain key frames from the reference view together with DCP-coded frames from another view, so as to display another view only or alternate between the two views. The latter is more flexible but involves more complicated data scheduling. A further extension is to the multi-view (or free-viewpoint) video, where more than two cameras record the same video from each different angle. This would allow users to arbitrarily select one viewpoint of the screen to enjoy the video, not necessary to be on a fixed viewing position in the middle front of the screen. It also enables stereoscopic display without wearing special glasses. Our P2P streaming system is flexible in supporting multi-view stereo streaming as stated previously. Nevertheless, given the high degree of view diversity and dynamics, more advanced multi-view design (e.g., overlay construction, partnership maintenance) are to be further developed.

Chapter 4

Evaluation

4.1 Simulation Setup

We evaluate the performance of our 3D/multi-view video streaming system through simulations. Similar to [22], we generate three typical classes of peers, namely, Cable/Ethernet, DSL2, and Modem/ISDN/DSL1. We summarize the bandwidth distribution and peer population for each class in Table 4.1. Due to the existence of free riders in traditional peer-to-peer systems, we assume that peers are willing to contribute approximately half of their resources (download bandwidth) for sharing. As in previous studies [36] [56], we assume a Poisson process with rate λ for peer arrival, and the default λ is set to 20, i.e., on average 20 peers arrive every minute (we will examine the impact of peer arrival rate in later subsections). We also use a Weibull distribution to model the lifetime of the participating peers [18]. As such, the peers join the system at different times, and would stay throughout the simulation (60 minutes) or depart earlier should a peer has a relatively short lifetime.

The video source we used for simulation is based on the standard multi-view video sequence "Ballet" (MERL [5]). The resolution is 1024*768 with a frame rate of 15 frames/s. We select two views to construct a stereo video sequence of 120 seconds. Using the reference JMVC 8.0 Encoder [4], adjacent two view video has an average bitrate of 746.4kbps, and we repeat the sequence throughout the 1-hour simulation.

Table 4.1: Bandwidth capacity and peer distribution

Class	Population	Download	Upload
Cable/Ethernet	60%	3Mbps	1.5Mbps
DSL2	20%	1.5Mbps	768Kbps
Modem/ISDN/DSL1	20%	768Kbps	384Kbps

4.2 3D Video Performance

In this Section, we consider a fixed viewpoint of 3D/stereo streaming. We firstly evaluate the feasibility as well as the benefit of our proposed separate streaming system in 4.2.1. Performance comparison between our proposed schedulers and the optimal scheduler, as well as the state-of-the-art of existing schedulers is conducted in 4.2.3. Finally, we study some impact factors on our scheduling algorithm in 4.2.4.

4.2.1 Sep-Streaming vs. Mix-Streaming

To evaluate our separated streaming, a typical P2P mesh for 2D video is implemented as a baseline for comparison, where to accommodate 3D video, the two streams are simply mixed together with a random scheduler (referred as Mix_R). Our separated streaming also implements a random scheduler (referred as Sep_R). In both systems, buffer window size is set to be 20 (in terms of the number of segments). Peers have the default arrival rate ($\lambda = 20$). During streaming peers have totally eight serving partners, and upon bad partners, peers would update partners list from server, and finally fail if no good partners updated after several rounds unfortunately.

Figure 4.1(a) shows the average streaming rate of all active peers for the overlay of different sizes. Note that we consider a dynamic system here. That is, the overlay size will generally increase when time increases because of continuous new-coming and leaving peers. When our simulation approaches the end (time=60min), we have more than 1000 active peers totally in the streaming overlay. We record the average rate at each simulation minute, and plot sampled minutes in the Figure. As we stated in previous section, the original video has a data rate of approximately 746.4kbps. We can see that there is a gap between the original rate and both systems'. This is because we compute the average data rate of all peers, which includes new joined peers (those are in the startup stage, and have not received enough amount of data to begin playback) and failed peers (those have large

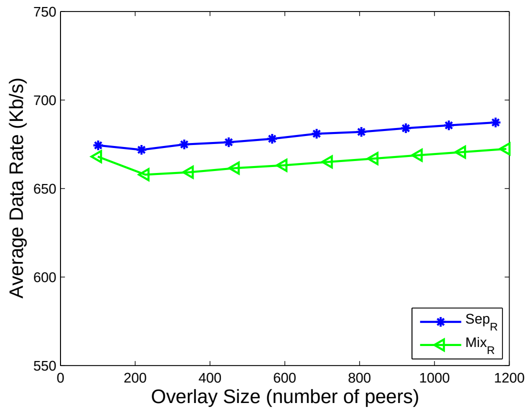

(a) Average data rate

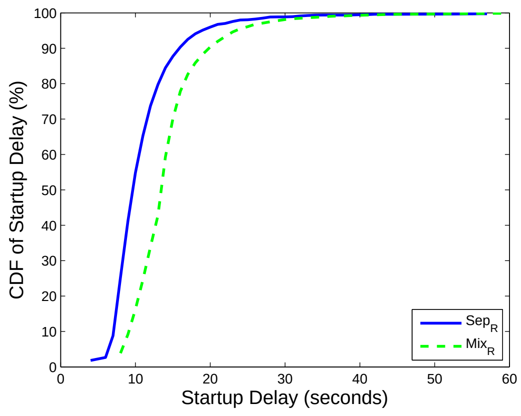

(b) Startup delay

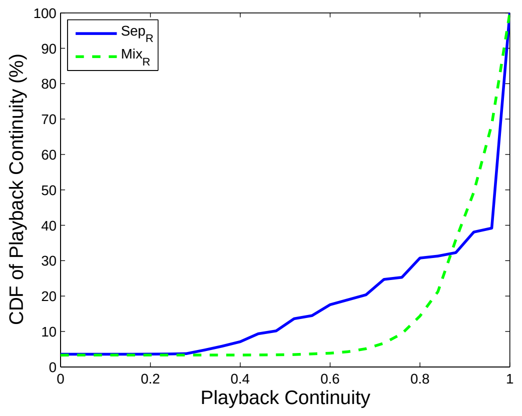

(c) Playback continuity

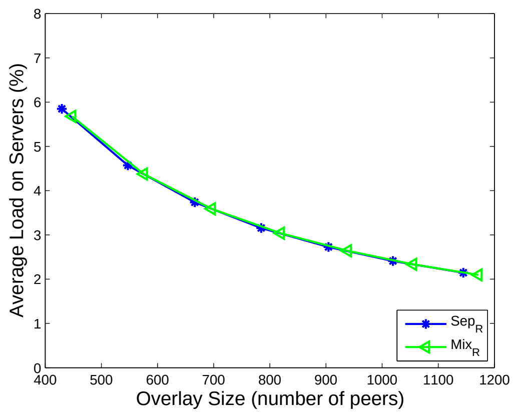

(d) Server load

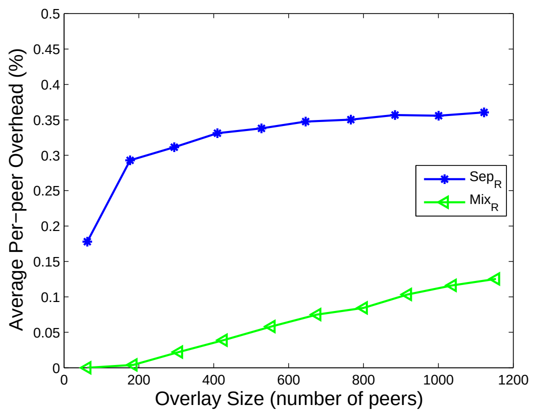

(e) Per-peer overhead

Figure 4.1: The feasibility and benefit of separate streaming

playback delays, and simply stuck during some playback position). Another reason for the gap is the coexistence of peer bandwidth heterogeneity and content distribution. That is, powerful peers may lack of available content while peers with rich content suffer from bandwidth bottleneck. And thus, peer upload bandwidth (the average upload is 1152Kbps, which can only reach 1.5 of the streaming rate) may not be fully utilized due to the poor content distribution, which is known as a challenge in peer-to-peer networks (this discussion is out of the scope of this thesis). As we will see later, the optimal scheduler can not achieve the original streaming rate either. When the overlay becomes stable, Sep-streaming performs better than Mix-streaming with a noticeable improvement (around 10Kbps). This implies that our separated streaming design not only provides better streaming flexibility but also comparable/higher streaming rate.

The cumulative distribution function (CDF) of the startup delay and playback continuity are depicted in Figure 4.1(b) and Figure 4.1(c) respectively. In our simulation, the initial buffering time is set to 10 seconds, i.e., a peer can only start playing videos after 10 seconds of video segments are downloaded. We can see from the figure that Mix_R has approximately 50% peers have startup delay of less than 15 seconds. However, Sep_R reduces the delay to 10 seconds with the same peer population, which means that for those peers, they could receive the first 10 seconds amount of data, and begin playback with 5 seconds less of the time, which is noticeable during the buffering stage.

We also investigate the playback quality experienced by individual peers, particularly, the continuity of the streaming playback as represented by the fraction of the on-time segments [62]. In our comparison, these on-time segments not only need to catch up their deadlines, but also, they have to be paired (or valid) as single left segment or single right segment will fail to constitute a stereo perception (in the Mix-streaming case, received data are all already valid). The CDF of playback continuity for all peers is plotted in Figure 4.1(c), which shows that, near 80% of the peers enjoy a continuity over 0.8 in Mix_R while only 70% peers have the same continuity in Sep_R. However, Sep_R has more peers with higher continuity (e.g., Sep_R has more than 60% peers with continuity of 0.96 while Mix_R only have 35% peers achieving this level). The better performance of Mix_R in the lower continuity range is because all received segments in Mix-streaming are considered to be valid while in Sep_R, unsynchronized segments are regarded to be useless for continuity improvement, which results in increased invalid segments (or worse playback continuity). This implies that more advanced scheduling algorithm is to be developed to synchronize segments in Sep-streaming.

To this end, our separated streaming design not only provides better streaming flexibility but also comparable/better streaming service. We now compare the system cost in terms of server load and peer control overhead for the two systems. As shown in Fig.4.1(d), server load is alleviated to a low level by Sep-streaming and confirms its scalability. Fig.4.1(e) shows that Sep-streaming has higher peer overhead than Mix-streaming, which is due to the distribution of additional 3D related information (e.g., view index).

4.2.2 Comparison with Optimal

We implement the MIQP solver of CPLEX to get the optimal scheduling (referred as `OPT` algorithm), serving as a benchmark for performance comparison with the two proposed algorithms (`BMF` and `HPF`).

Figure 4.2(a) shows the average streaming rate comparison with dynamic overlay (to see clearly, we scale the Y axis to a smaller range of data rate). As we see that both `BMF` and `HPF` algorithms achieve near-optimal streaming rate, with only 10Kbps gap to the optimal. Further, the two can run much faster than the `OPT` (in our simulation, they only spent 1/250 time of OPT did), which confirms their efficiency to support real time streaming. Surprisingly, the optimal scheduling introduces higher server load than the two, see Figure 4.2(b). We believe that this is due to the unbalanced workload among partners, which results in some peers having bad partners and finally they resort to the server for data transmission. We also see from the two figures that `BMF` achieves a slightly higher streaming rate than `HPF` algorithm. This is because, although `BMF` has no performance guarantee for the stereo segment scheduling, it performs well on most cases. The worst case only happens with some specific partner bandwidth and availability distribution, as well as peer's specific segment demand, which however turns out to rarely happen in P2P streaming system according to the above observation.

4.2.3 Comparison with Other Schedulers

Since `BMF` and `HPF` achieve very similar streaming service, we pick `BMF` to compare with two other existing schedulers. There are no scheduling algorithms in the existing literature that are specifically designed for stereo segment, we thus select two 2D scheduling algorithms which are used in popular P2P streaming systems currently, namely the Rarest First (`RF`)

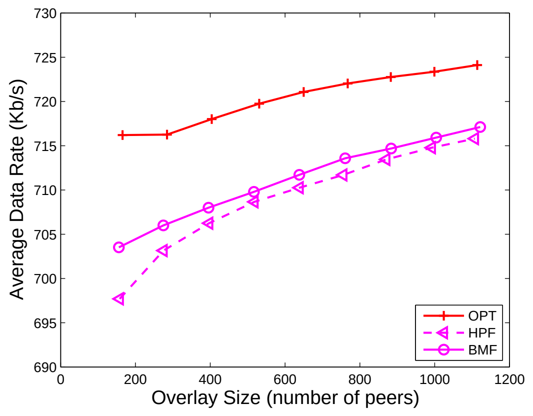

(a) Average data rate

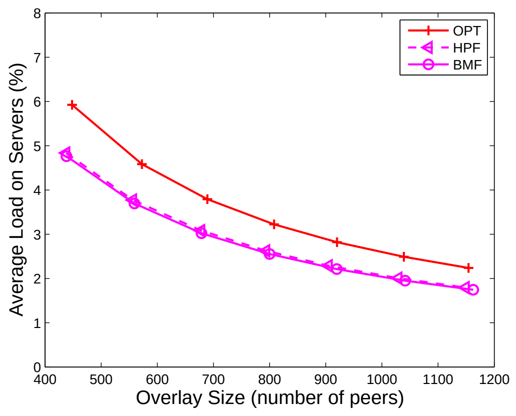

(b) Server load

Figure 4.2: Performance comparison of the optimal (OPT) and the two proposed algorithms (BMF and HPF)

scheduling [62], and the Random (`Random`) scheduling [37]. The `Random` algorithm schedules segment randomly from a random partner, and the `RF` algorithm selects the segment with the fewest number of partners to schedule first and so on. Among multiple partners with the same number of the desired segment, the scheduler selects the partner with the highest bandwidth. With the default setting (peer arrival rate=20 peers/min, buffer window size=20 segments), we firstly compare the user experience (streaming rate, startup delay, playback continuity and media synchronization) and system cost (server load and per-peer overhead). We then vary the peer arrival rate and window size to see the impact on the three systems.

As before, we depict the average data rate in Figure 4.3(a) for overlay with dynamic sizes. We plot the data rate when the system can self-serve through peer-to-peer computing without help of the server and reach a stable streaming. As we can see that `RF` and `Random` have comparable streaming rate while `BMF` achieves much better performance with an approximately 30Kbps higher (equally 4% improvement). This is because both of `RF` and `Random` schedule segments regardless of differentiation of segment importance and synchronization among different views, which result in more important segments missing or many received segments useless for playback. Further, the random nature of the `Random` scheduler fails to consider the heterogeneity of upload bandwidth and content distribution among partners when scheduling, and thus it has even lower streaming rate than the `RF` scheduler.

Figure 4.3(b) shows the CDF of startup delays for the three schedulers. We find that all of the three yield very similar distribution of startup delay with `BMF` slightly better. The playback continuity comparison (Figure 4.3(c)) shows that near 80% peers achieve more than 0.8 continuity with `BMF` while they have 70% peers with the same level of the continuity in `RF` and `Random`. The reason is similar to the streaming rate, where the random scheduling and the rarest strategy lack of synchronization among different views, which results in increased invalid segments (or worse playback continuity). To further verify the synchronization of our scheduler, we compare the synchronization index in Figure 4.3(d). The *synchronization index* is defined as the number of received segment pairs over the accumulated number of received pairs and received single segments (only left segment or right segment is received, which means that they are not successfully synchronized). The figure shows that with `BMF` scheduler, the system could have much higher synchronization index that the other two, demonstrating the superiority of differentiating the importance and dependency of data segments. Specifically, for `RF` and `Random`, only 65% users receive 90% successfully paired segments, and the `BMF` has more than 95% peers that can achieve almost all segments synchronized.

We next evaluate server load and peer maintenance overhead in Figure 4.3(e) and Figure 4.3(f) respectively. All three systems relieve server load to a contribution level of less than 3%, while `BMF` can save server capacity of approximately 0.5% more comparing to the other two. This means that in a streaming system where server has limited capacity, `BMF` can either improve the streaming quality (in terms of data rate) for the same peer population or accommodate more peers with the same streaming quality. Peer maintenance overhead is computed when peers exchange buffer bitmap to indicate data availability, respond to requests (e.g., partnership establishment, data downloading etc.) and deal with dynamics. We can see that both `RF` and `Random` have higher overhead (by 15% more) than `BMF`. We believe that this is due to the higher frequency of updating parents list, which results from poor performance of `RF` and `Random`.

We are also interested in how the buffer window size influences the viewing experience on the three systems. Figure 4.4 shows the average data rate with different window sizes, scaling from 5 segments to 25 segments. We can find that smaller window sizes (sizes of 5 and 10) produce relatively lower streaming rate than the higher values, and the rate goes stable afterwards when the window size reaches a value of 15. We believe that this is because

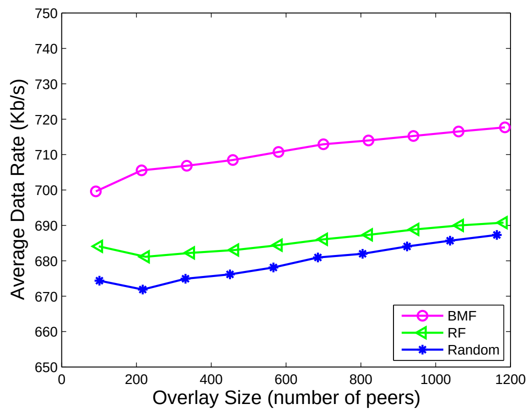

(a) Average data rate

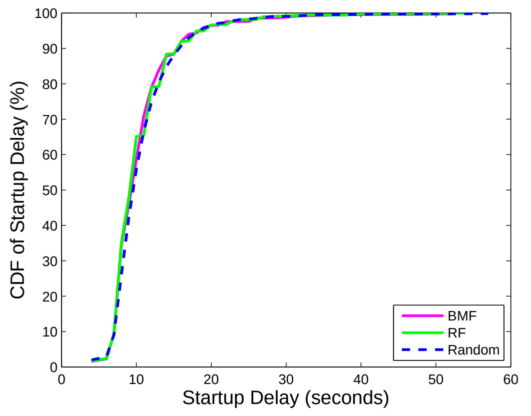

(b) Startup delay

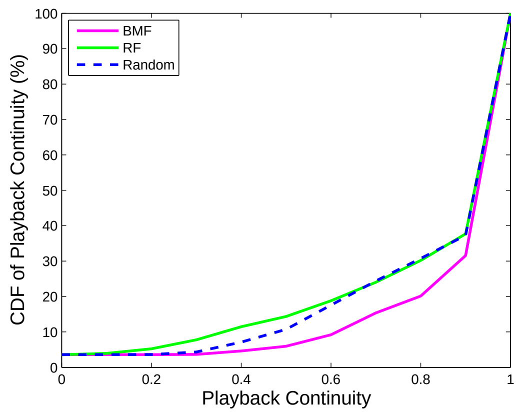

(c) Playback continuity

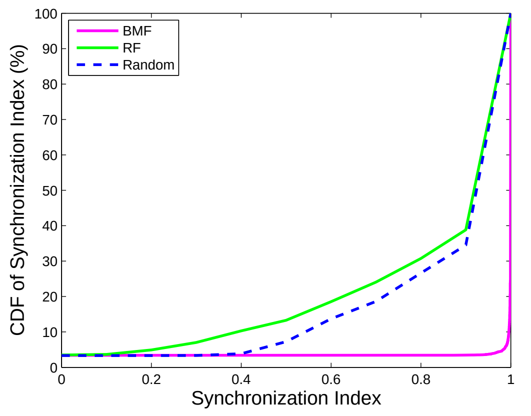

(d) Synchronization index

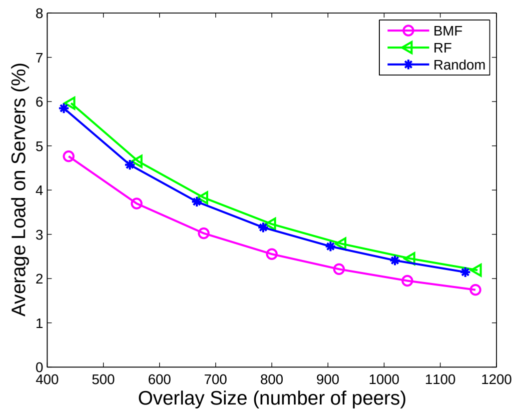

(e) Server load

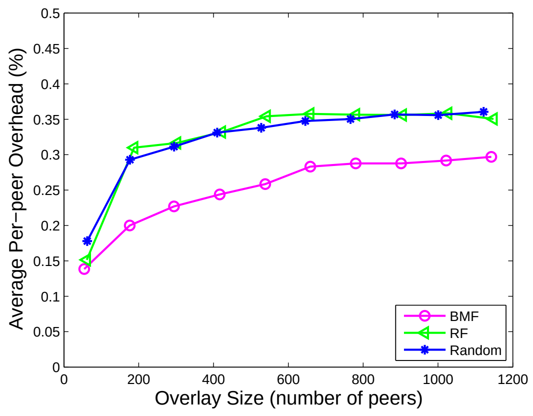

(f) Per-peer overhead

Figure 4.3: Performance comparison of the proposed BMF algorithm and two other popular algorithms (RF and Random)

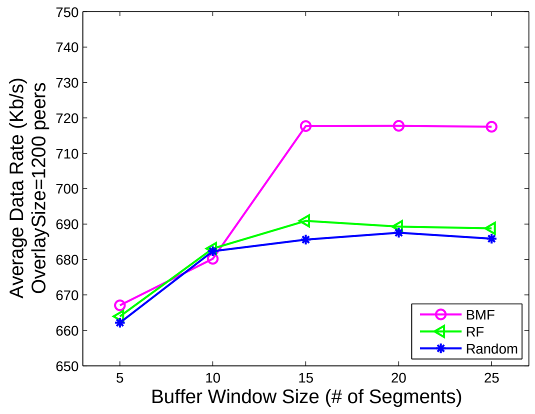

Figure 4.4: Impact of buffer window sizes

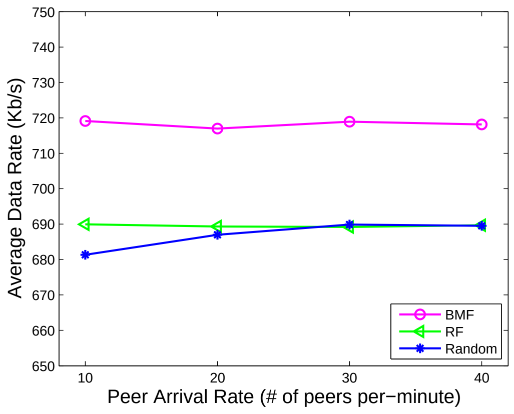

Figure 4.5: Impact of peer arrival rates

a smaller window would probably receive insufficient amount of segments for playback; on the other hand, a too large window size could not improve system performance since the peers might not be able to well schedule all the segments with limited resources (i.e., the average upload bandwidth one peer could receive is bounded by a consistent value). The remarkable data rate gap in `BMF` when the window size increases from 10 to 15 is because the size reaches the frame rate which is 15 frames/s. Since the buffer slides forward and also consumes received segment every second, size value close to the consuming rate will probably reach the maximum streaming rate as long as the scheduler can fulfill the buffer for each second. This further verifies the efficiency of `BMF`.

Finally, we examine the influence of peer arrival rate in Figure 4.5 (the buffer window size is fixed to 20 segments). The observation is that `BMF` performs stably with different peer arrival rates as the existing state-of-the-art of schedulers, and it however provides much higher streaming rate, which is already confirmed in the previous figures. We thus conclude that system with `BMF` provides better streaming quality, stable performance and scales well.

4.2.4 Impact of Partner Sorting

While `BMF` performs well, there is one key factor that may influent on its performance, which is the partner sorting. This is because `BMF` algorithm process one partner in each round with no later partner information considered in the current processing round. We now implement two partner sorting mechanisms to study the impact, namely `bwDecreasing` and `segIncreasing`. The `bwDecreasing` sorts peer's partners with their available bandwidth in decreasing order. That is, peer will select the partner to process scheduling with the highest bandwidth first till to the lowest one. And the `segIncreasing` sorts the partner according to their available total number of segments that peer wants, following the increasing order. We use these two sorting methods because the available bandwidth and segments availability are two key constraints in scheduling, with the first one serves to better utilize the bandwidth, and the second one tries to balance the segment distribution (processes partner with the rarest segment first).

Similarly, we pick the streaming rate as the system service and server load, per-peer overhead as the system cost. Figure 4.6(a) shows that the sorting mechanisms have little impact on the streaming quality of `BMF` scheduler, which implies that our scheduling algorithm performs well independently of the processing ordering. Scheduler with `bwDecreasing` sorting brings slightly higher streaming rate (about 2Kbps higer), this is, however, due to the help from server; see Fig.4.6(b). Besides the aggravated server load, the sorting mechanisms introduce higher per-peer overhead (by at least 15%, see Fig. 4.6(c)). We thus believe that our pure `BMF` can provide comparable streaming services with lower system cost.

4.3 Multi-view Stereo with View Change

In this section, we evaluate our V-Plane overlay (`H-VO`) for the multi-view video with view change, and compare both the streaming quality and system cost with a random mesh overlay (`H-RO`). In both systems, we implement our `BMF` heuristic with default simulation setting (number of direct partners=8, buffer window size=20 segments, peer arrival rate=20 peers/min). To support multi-view video, we consider a scenario consisting of totally four 2D views (and thus supporting totally three 3D/stereo viewpoints, each from two adjacent views). Upon joining, each peer randomly selects one viewpoint to enjoy, and during watching, it will change its viewpoint once (in a random fashion) and afterwards continues watching to the end. For `H-VO`, peers maintain a uDP list consisting of indirect partners. We pick the streaming rate, startup delay and playback continuity to evaluate the streaming quality (since they produce almost the same synchronization index, we skip evaluation of this metric here), and the system cost between `H-VO` with different sizes of uDP lists and `H-RO`.

As we can see in Figure 4.7(d) that `H-VO` can reduce more server traffic. This is because in `H-RO`, view changing peers failed to locate new partners for several rounds and finally

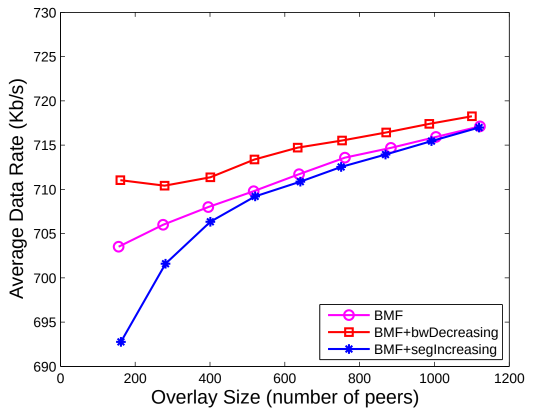

(a) Average data rate

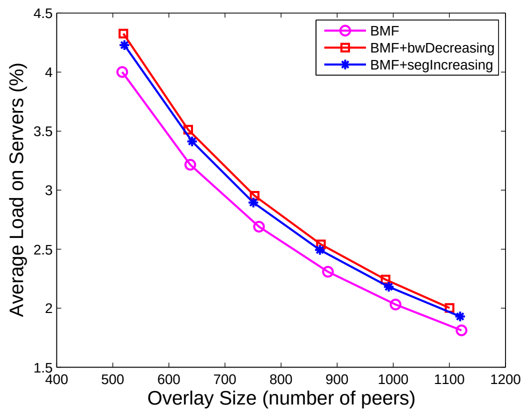

(b) Server load

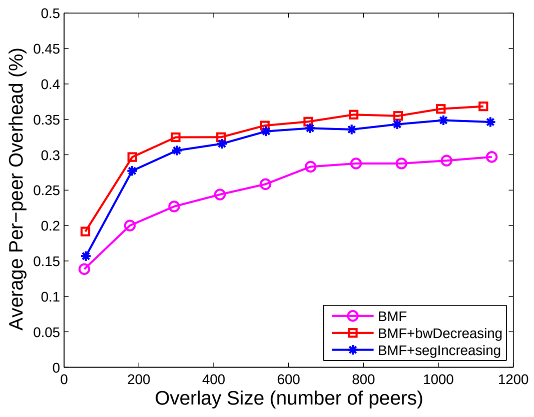

(c) Per-peer overhead

Figure 4.6: Impact of partner sorting on BMF performance

resort to server for transmission. The help from the server results in better data rate and playback continuity in H-RO, which is comparable to `H-VO` with uDP size of 18, as shown in Figure4.7(a), 4.7(b) and 4.7(c). However, `H-VO` (uDP=18) has remarkably less traffic from server, which indicates that our `H-VO` copes well with view change without relying on server, and thus scales better. Maintenance of uDP list would introduce not much extra overhead in peers since there is no data transmission between indirect partners (thus, no bitmap or connection cost consumed). However, they do increase the server load as maintaining uDP list requires increased query/transmission when a peer first joins the system or updating uDP list upon bad viewing experience.

The performance of different sizes of uDP list can be seen from these figures as well. As we have totally three stereo viewpoints and a DP size of 8, we believe that the uDP size of approximately 16 is sufficient for quickly locating new partners in the case of view change, given that a peer will randomly select one of the other two viewpoints to watch. Intuitively, more indirect partners maintained, higher probability of new partners will be located, and better quality (streaming rate, startup delay and playback continuity) a peer will experience during view change. And the server load increases as uDP size grows due to the the increased query/transmission for more indirect partners. Surprisingly, peer overhead generally decreases when uDP size scales. We believe that this is because, the better streaming quality brought by more indirect partners maintained eliminates the frequent update of bad partners upon viewpoint change, which results in fewer bitmap/messages exchanged (or lower control overhead).

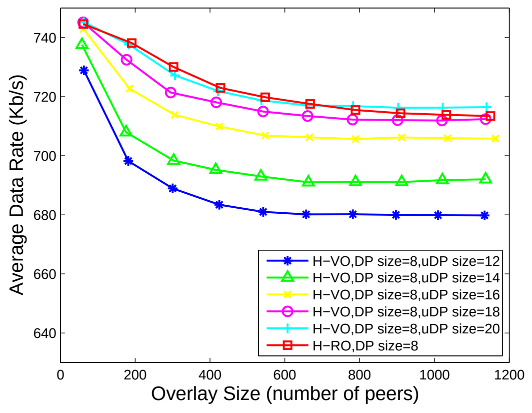

(a) Average data rate

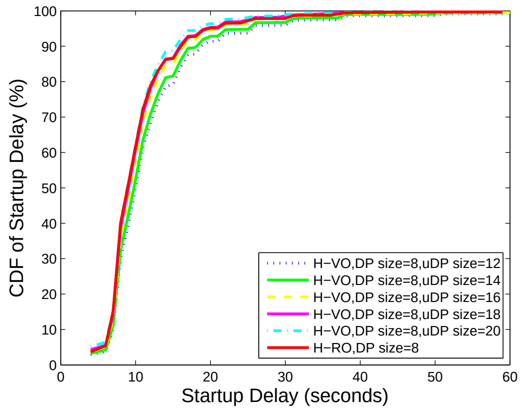

(b) Startup delay

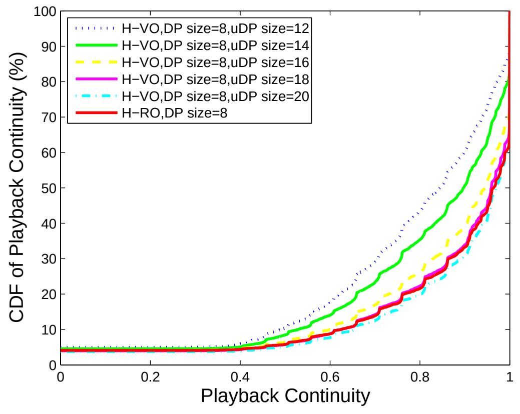

(c) Playback continuity

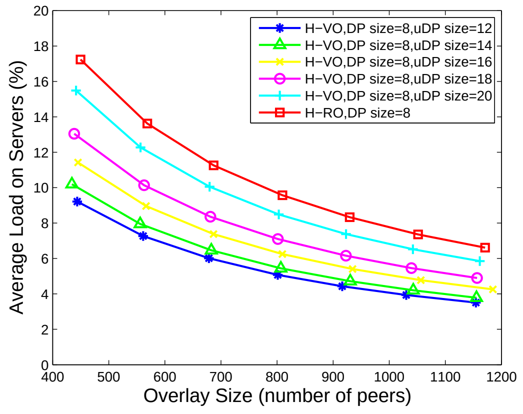

(d) Server load

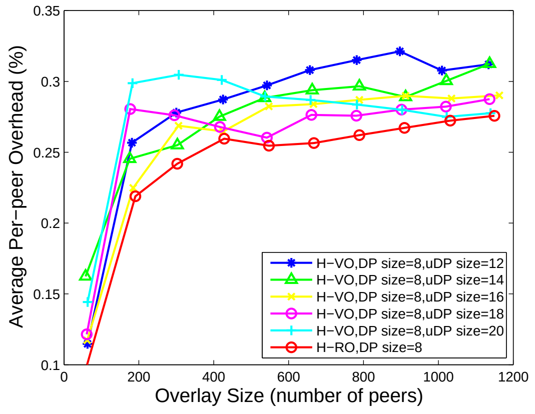

(e) Per-peer overhead

Figure 4.7: Multi-view stereo with view change and the impact of uDP size

Chapter 5

Conclusion and Future Work

This thesis offered a preliminary study on efficient streaming of 3D/multi-view videos over peer-to-peer networks. We focus on the segment scheduler design, which is the key component in peer-to-peer streaming systems. We demonstrated that the inherent multi-stream nature of stereo video makes segment scheduling more difficult, particularly with the existence of multiple senders in a peer-to-peer overlay. We mathematically formulate the stereo segment scheduling as a BQP problem to maximize the number of weighted segment pairs, which is NP-Hard. Given the stringent playback requirement in real time video streaming, the optimal solution is too computationally costly to obtained. We thus develop two heuristics to efficiently update the scheduling. With theoretical analysis and simulation, we show that the proposed algorithms achieve near-optimal performance and outperforms other popular algorithms. We further extend the design to support multi-view video.

There are a number of possible future avenues to explore. We are currently working on more advanced weight modeling of the segment pair based on the rate-distortion model. Besides, we continue on developing the overlay design to fully support multi-view with more views and higher view diversity/dynamics. We are also interested in building and experimenting prototypes with the H.264 MVC codec on on-demand streaming with 3D/multi-view video.

Bibliography

[1] BitTorrent. http://www.bittorrent.com/.

[2] Gnutella. http://www.gnutella.com/.

[3] ILOG CPLEX. http://www.ilog.com/products/cplex/.

[4] Joint Multiview Coding (JMVC) 8.0. garcon.ient.rwthaachen.de.

[5] MERL. http://www.merl.com/.

[6] PPLive. http://www.pplive.com/.

[7] UUSee. http://www.uusee.com/.

[8] A. Aksay, S. Pehlivan, E. Kurutepe, C. Bilen, T. Ozcelebi, G.B. Akar, M.R. Civanlar, and A.M. Tekalp. End-to-end Stereoscopic Video Streaming with Content-adaptive Rate and Format Control. *Signal Processing: Image Communication*, 22(2):157–168, 2007.

[9] S. Banerjee, B. Bhattacharjee, and C. Kommareddy. Scalable Application Layer Multicast. In *Proc. of ACM SIGCOMM'02*.

[10] F. Boronat, J. Lloret, and M. García. Multimedia Group and Inter-stream Synchronization Techniques: A Comparative Study. *Information Systems*, 34(1):108–131, 2009.

[11] Bin Chang, Liang Dai, Yi Cui, and Yuan Xue. On Feasibility of P2P On-Demand Streaming via Empirical VoD User Behavior Analysis. In *Proc. of ICDCS'08 Workshop*.

[12] Bin Cheng, Lex Stein, Hai Jin, Xiaofei Liao, and Zheng Zhang. GridCast: Improving Peer Sharing for P2P VoD. *ACM Transactions on Multimedia Computing, Communications and Applications*, 4(4):1–31, October 2008.

[13] X. Cheng, F. Wang, J. Liu, and K. Xu. Collaborative Delay-aware Scheduling in Peer-to-Peer UGC Video Sharing. In *Proc.of NOSSDAV'10*.

[14] P.A. Chou, H.J. Wang, and V.N. Padmanabhan. Layered Multiple Description Coding. In *Proc. of PV'03*.

[15] Y. Ding, J. Liu, D. Wang, and H. Jiang. Peer-to-Peer Video-on-Demand with Scalable Video Coding. *Computer Communications*, 33(14):1589–1597, 2010.

[16] Y. Guo, C. Liang, and Y. Liu. AQCS: Adaptive Queue-based Chunk Scheduling for P2P Live Streaming. In *Proc. of IFIP'08.*

[17] T. Hashimoto and Y. Ishibashi. Group Synchronization Control over Haptic Media in a Networked Real-time Game with Collaborative Work. In *Proc.of ACM SIGCOMM NetGames '06.*

[18] Y. He, G. Siganos, M. Faloutsos, and S. Krishnamurthy. A Systematic Framework for Unearthing the Missing Links: Measurements and Impact. In *Proc. of NSDI'07.*

[19] C.H. Hsu and M. Hefeeda. Quality-aware Segment Transmission Scheduling in Peer-to-Peer Streaming Systems. In *Proc. of ACM MMSys'10.*

[20] Shun-Yun Hu, J.-R. Jiang, and Bing-Yu Chen. Peer-to-Peer 3D Streaming. *IEEE Internet Computing*, 14(2):54–61, 2010.

[21] S.Y. Hu, T.H. Huang, S.C. Chang, W.L. Sung, J.R. Jiang, and B.Y. Chen. FloD: A Framework for Peer-to-Peer 3D Streaming. In *Proc.of IEEE INFOCOM'08.*

[22] C. Huang, J. Li, and K.W. Ross. Can Internet Video-on-Demand be Profitable? In *Proc. of ACM SIGCOMM'07.*

[23] Z. Huang, W. Wu, K. Nahrstedt, A. Arefin, and R. Rivas. TSync: A New Synchronization Framework for Multi-site 3D Tele-immersion. In *Proc.of NOSSDAV'06.*

[24] Y. Ishibashi and S. Tasaka. A Synchronization Mechanism for Continuous Media in Multimedia Communications. In *Proc.of IEEE INFOCOM'95.*

[25] T.V. Johnson and A. Zhang. Dynamic Playout Scheduling Algorithms for Continuous Multimedia Streams. *Multimedia Systems*, 7(4):312–325, 1999.

[26] K. Katayama and H. Narihisa. Performance of Simulated Annealing-based Heuristic for The Unconstrained Binary Quadratic Programming Problem. *European Journal of Operational Research*, 134(1):103–119, 2001.

[27] P. Kauff, N. Atzpadin, C. Fehn, M. Muller, O. Schreer, A. Smolic, and R. Tanger. Depth Map Creation and Image-based Rendering for Advanced 3DTV Services Providing Interoperability and Scalability. *Signal Processing: Image Communication*, 22(2):217–234, 2007.

[28] E. Kurutepe, A. Aksay, C. Bilen, C.G. Gurler, T. Sikora, G.B. Akar, and A.M. Tekalp. A Standards-based, Flexible, End-to-End Multi-view Video Streaming Architecture. In *Proc. of PV'07.*

[29] E. Kurutepe, M.R. Civanlar, and A.M. Tekalp. Interactive Transport of Multi-view Videos for 3DTV Applications. *Journal of Zhejiang University Science*, 7(5):830–836, 2006.

[30] E. Kurutepe, M.R. Civanlar, and A.M. Tekalp. Client-Driven Selective Streaming of Multiview Video for Interactive 3DTV. *IEEE Transactions on Circuits and Systems for Video Technology*, 17(11):1558–1565, October 2007.

[31] E. Kurutepe and T. Sikora. Feasibility of Multi-view Video Streaming over P2P Networks. In *Proc. of 3DTVCON'08*.

[32] E. Lamboray, W. Stephan, et al. Real-Time Streaming of Point-based 3D Video. In *Proc. of IEEE VR'04*.

[33] D.T. Lee. On k-Nearest Neighbor Voronoi Diagrams in The Plane. *IEEE Transactions on Computers*, 100(6):478–487, 1982.

[34] B. Li, G.Y. Keung, S. Xie, F. Liu, Y. Sun, and H. Yin. An Empirical Study of Flash Crowd Dynamics in a P2P-based Live Video Streaming System. In *Proc. of IEEE GLOBECOM'08*.

[35] L. Li, A. Karmouch, and ND Georganas. Real-time Synchronization Control in Multimedia Distributed Systems. *ACM SIGCOMM Computer Communication Review*, 22(3):79–87, 1992.

[36] Taoyu Li, Minghua Chen, Dah-Ming Chiu, and Maoke Chen. Queuing Models for Peer-to-peer Systems. In *Proc. of IPTPS'09*.

[37] C. Liang, Y. Guo, and Y. Liu. Is Random Scheduling Sufficient in P2P Video Streaming? In *Proc. of ICDCS'08*.

[38] J. Liu, S.G. Rao, B. Li, and H. Zhang. Opportunities and Challenges of Peer-to-Peer internet Video Broadcast. *Proceedings of the IEEE*, 96(1):11–24, January 2008.

[39] K. Lua, J. Crowcroft, M. Pias, R. Sharma, and S. Lim. A Survey and Comparison of Peer-to-Peer Overlay Network Schemes. *IEEE Communications Survey and Tutorial*, 7(2):72–93, 2004.

[40] N. Magharei and R. Rejaie. Prime: Peer-to-Peer Receiver-drIven MEsh-based Streaming. *IEEE/ACM Transactions on Networking*, 17(4):1052–1065, 2009.

[41] W. Matusik and H. Pfister. 3D TV: a Scalable System for Real-Time Acquisition, Transmission, and Autostereoscopic Display of Dynamic Scenes. In *Proc. of ACM SIGGRAPH'04*.

[42] JVT of MPEG and ITU-T. Joint Draft 7.0 on Multiview Video Coding (JVT-AA209). Augest 2008.

[43] D.E. Ott and K. Mayer-Patel. Coordinated Multi-streaming for 3D Tele-immersion. In *Proc. of ACM MM'04.*

[44] G. Petrovic et al. Near-Future Streaming Framework for 3D-TV Applications. In *Proc. of ICME'06.*

[45] S. Ramanathan and P.V. Rangan. Feedback Techniques for Intra-media Continuity and Inter-media Synchronization in Distributed Multimedia Systems. *The Computer Journal*, 36(1):19–31, 1993.

[46] S. Ratsanamy, P. Francis, M. Handley, R. Karp, and S. Shenker. A Scalable Content Addressable Network. In *Proc. of ACM SIGCOMM'01.*

[47] M. Saxena, U. Sharan, and S. Fahmy. Analyzing Video Services in Web 2.0: A Global Perspective. In *Proc. of NOSSDAV'08.*

[48] L. Smith. Space Perception and Parallax. *Philosophy*, 56(216):248–252, 1981.

[49] R. Steinmetz. Synchronization Properties in Multimedia Systems. *IEEE Journal on Selected Areas in Communications*, 8(3):401–412, 1990.

[50] I. Stoica, R. Morris, D. Karger, M.F. Kaashoek, and H. Balakrishnan. Chord: A Scalable Peer-to-Peer Lookup Service for Internet Applications. *ACM SIGCOMM Computer Communication Review*, 31(4):149–160, 2001.

[51] W.L. Sung, S.Y. Hu, and J.R. Jiang. Selection Strategies for Peer-to-Peer 3D Streaming. In *Proc.of NOSSDAV'08.*

[52] D. Tian and G. AlRegib. Multistreaming of 3D Scenes with Optimized Transmission and Rendering Scalability. *IEEE Transactions on Multimedia*, 9(4):736–745, 2007.

[53] D.A. Tran, K.A. Hua, and T. Do. Zigzag: An Efficient Peer-to-Peer Scheme for Media Streaming. In *Proc. of IEEE INFOCOM'03.*

[54] V. Venkataraman, K. Yoshida, and P. Francis. Chunkyspread: Heterogeneous Unstructured Tree-Based Peer-to-Peer Multicast. In *Proc. of IEEE ICNP'06.*

[55] F. Wang, Y. Xiong, and J. Liu. mTreebone: A Hybrid Tree/Mesh Overlay for Application-Layer Live Video Multicast. In *Proc. of ICDCS'07.*

[56] J. Wang, C. Yeo, V. Prabhakaran, and K. Ramchandran. On the Role of Helpers in Peer-to-Peer File Download Systems: Design, Analysis and Simulation. In *Proc. of IPTPS'07.*

[57] Y. Wang, Z. Wu, and J.M. Boyce. Modeling of Transmission-Loss-Induced Distortion in Decoded Video. *IEEE Transactions on Circuits and Systems for Video Technology*, 16(6):716–732, 2006.

[58] Y.-K. Wang and T. Schierl. RTP Payload Format for MVC Video. In *draft-wang-avt-rtp-mvc-05*.

[59] W. Wu, Z. Yang, I. Gupta, and K. Nahrstedt. Towards Multi-site Collaboration in 3D Tele-immersive Environments. In *Proc. of ICDCS'08*.

[60] X. Xin, SHI Yuanchun, GAO Yuan, and Q. Zhang. LayerP2P: A New Data Scheduling Approach for Layered Streaming in Heterogeneous Networks. In *Proc. of IEEE INFOCOM'09*.

[61] Z. Yang, B. Yu, K. Nahrstedt, and R. Bajscy. A Multi-stream Adaptation Framework for Bandwidth Management in 3D Tele-immersion. In *Proc.of NOSSDAV'06*.

[62] X. Zhang, J. Liu, B. Li, and T.S.P. Yum. CoolStreaming/DONet: A Data-driven Overlay Network for Efficient Live Media Streaming. In *Proc. of IEEE INFOCOM'05*.